Hadron Polarization

Frank Rathmann
Brookhaven National Laboratory

CFNS Summer School on Physics of the Electron-Ion Collider
June 14, 2024

Center for Frontiers in Nuclear Science

Brookhaven National Laboratory

frathmann@bnl.gov

Outline

1. Introduction: A Polarized Electron-Ion Collider
2. Polarized Particle beams
3. Hadron Polarimetry
4. Outlook / Summary

wiki.bnl.gov/EPIC/

1 Emerging Nucleons

How are gluons, sea quarks, and their intrinsic spins distributed in space and momentum in the nucleon?

Nuclear Physics **A1026** (2022) 122447

2 Nuclear Medium

How do colored quarks and gluons and colorless jets interact with the nuclear medium?

How does the nuclear environment affect quark and gluon distributions?

3 Gluon Saturation

What happens to the gluon density at high energy?

Are the properties of a saturated gluonic state universal among all nuclei?

The Electron-Ion Collider

- Variable center-of-mass energy:

$$\sqrt{s} = 20 - 140 \text{ GeV}$$

- Ion beams: protons, ^{3}He, Au, Pb, U
- High luminosity:

$$L = 10^{33} - 10^{34} \text{ cm}^{-1}\text{s}^{-1}$$

- **Polarized electron and proton beams:**

$$\boldsymbol{P \approx 70\%}$$


Current location of RHIC at Brookhaven National Lab

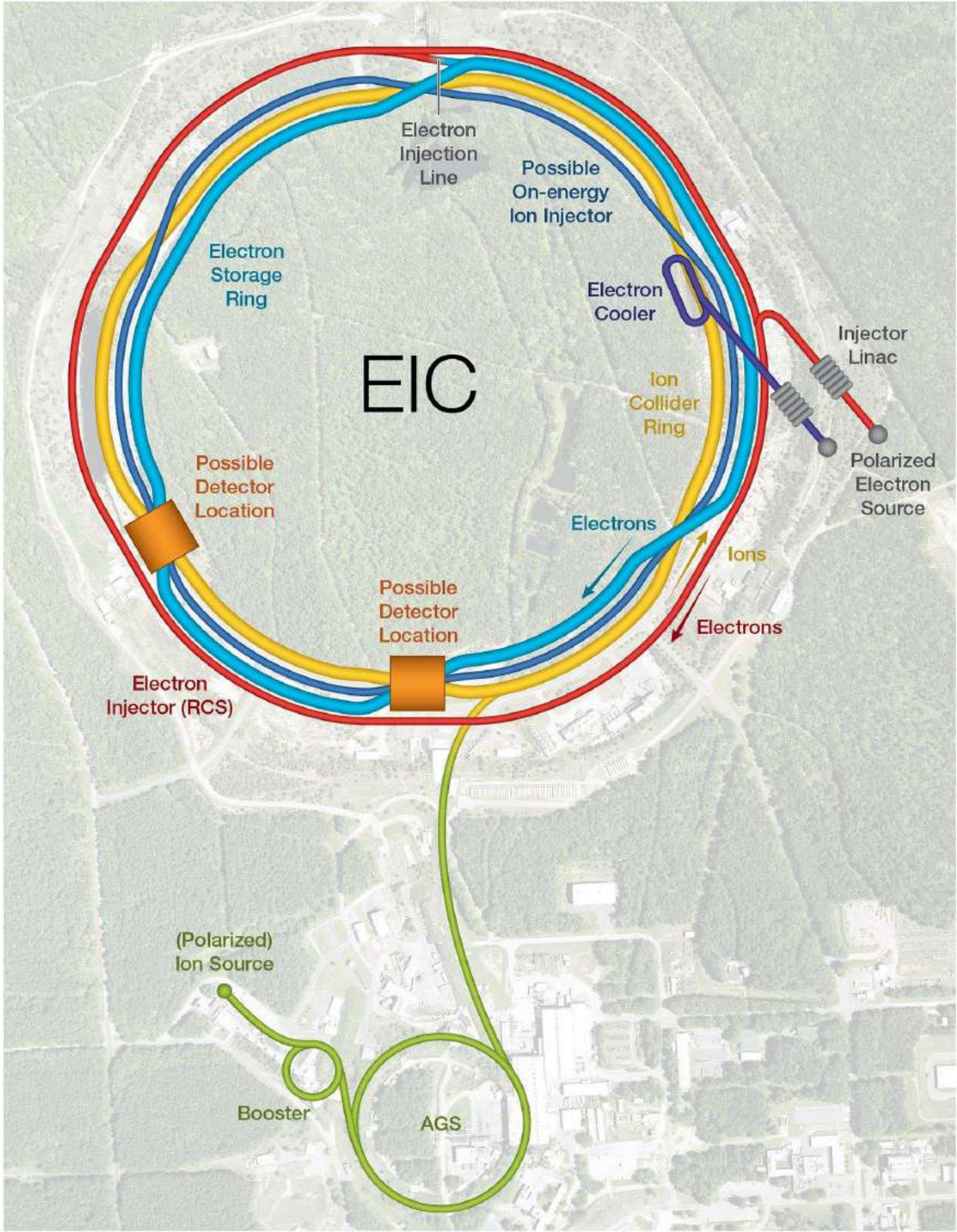

The Electron-Ion Collider

- Variable center-of-mass energy:

$$\sqrt{s} = 20 - 140\ \mathrm{GeV}$$

- Ion beams: protons, ^{3}He, Au, Pb, U
- High luminosity:

$$L = 10^{33} - 10^{34}\ \mathrm{cm^{-1}s^{-1}}$$

- **Polarized electron and proton beams:**

$$\boldsymbol{P \approx 70\%}$$

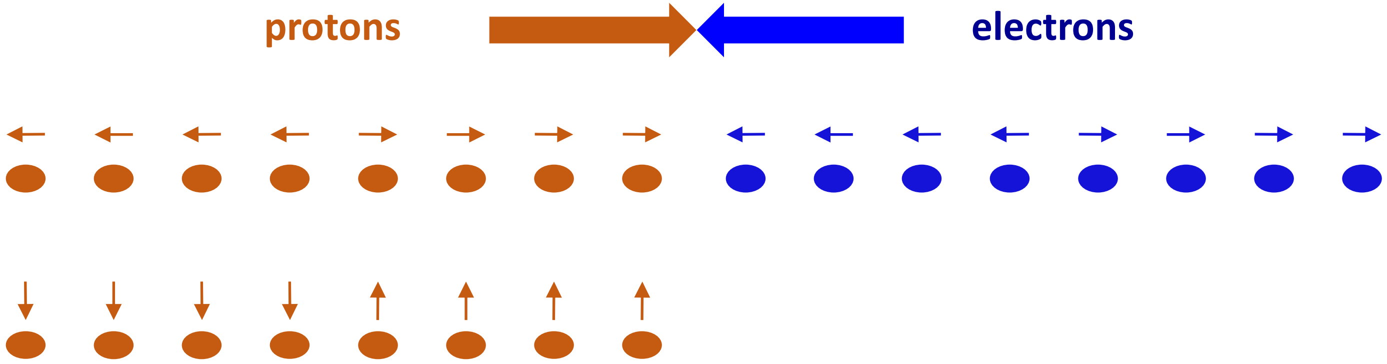

Electrons: $5 - 18$ GeV

Protons: $50 - 275$ GeV

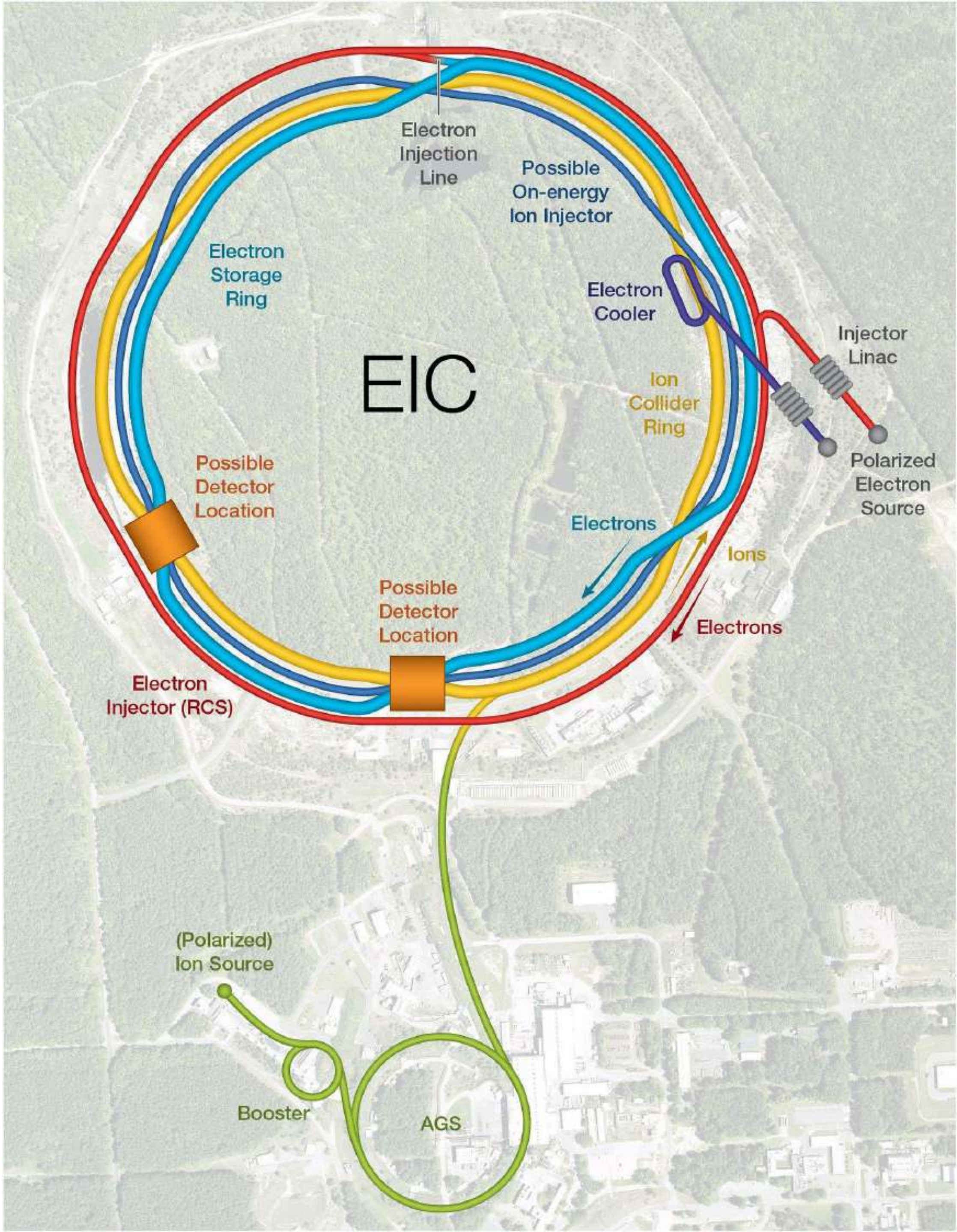

The Electron-Ion Collider

- Variable center-of-mass energy:

$$\sqrt{s} = 20 - 140 \text{ GeV}$$

- Ion beams: protons, ^{3}He, Au, Pb, U
- High luminosity:

$$L = 10^{33} - 10^{34} \text{ cm}^{-1}\text{s}^{-1}$$

- Polarized electron and proton beams:

$$P \approx 70\%$$

Electrons: $5 - 18$ GeV

Protons: $50 - 275$ GeV

But the energy of polarized protons leaving the source is only 10 keV…

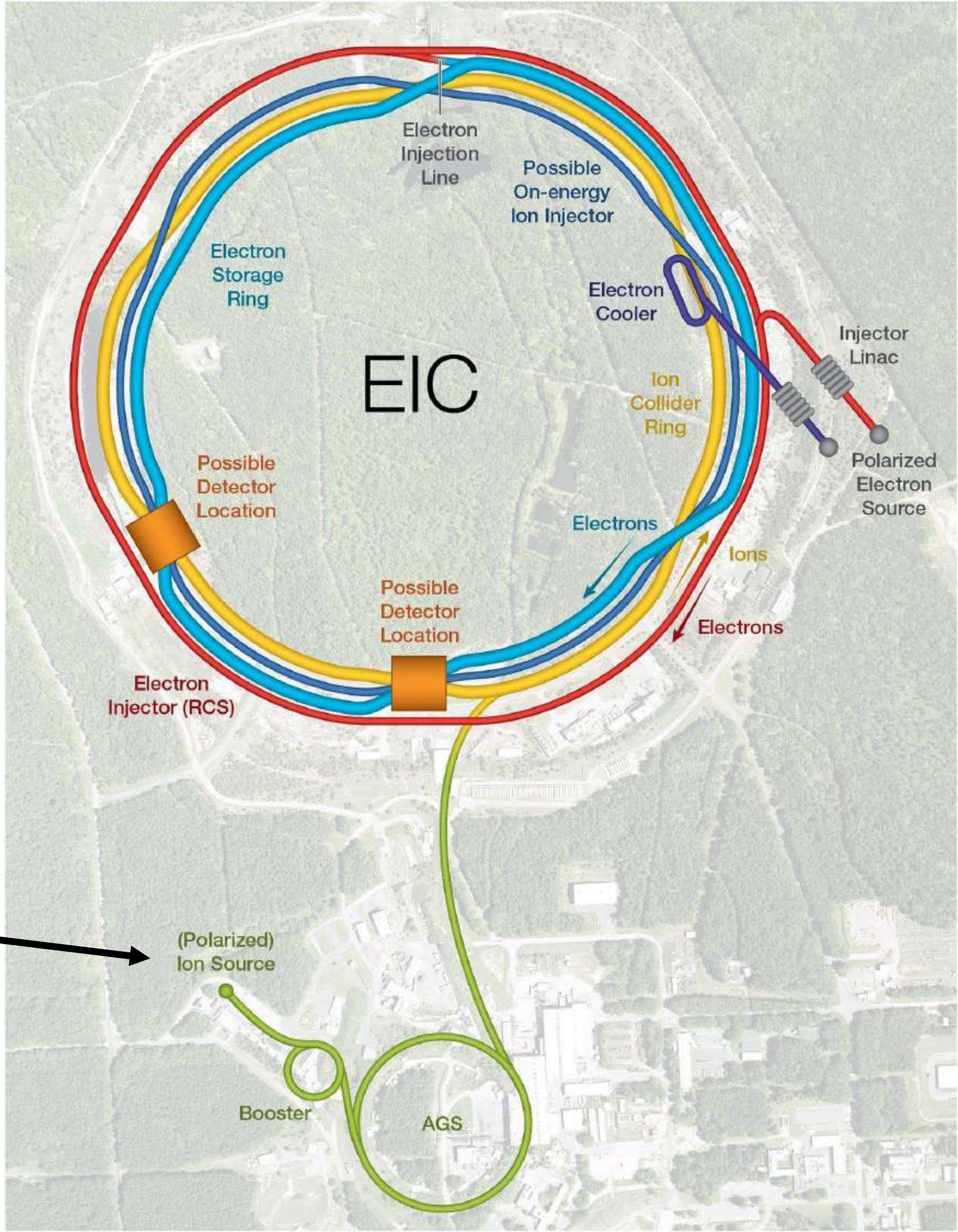

2. Polarized High Energy Particle Beams

1922 Stern-Gerlach experiment

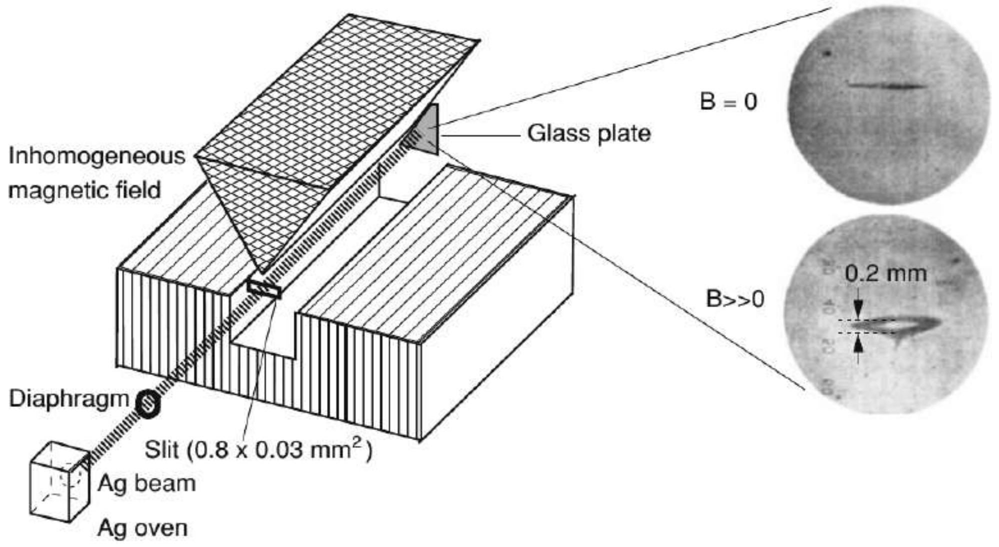

Setup and result of classical Stern-Gerlach experiment

Experiment showed for the first time the quantization of angular momentum:

- Quantization of new degree of freedom, later called electron spin.
- Interpretation was only put forward in 1927, 2 years after Goudsmit and Uhlenbeck found evidence of half-valued electron spin.
- Delay attributed to fact that Stern and Gerlach measured size of magnetic moment of Ag atom to be about $1\mu_B$ appropriate for orbital angular momentum $1\hbar$.
- Factor 2 compensating for factor $\frac{1}{2}$ in spin-$\frac{1}{2}\hbar$ particles (“Thomas factor”) was not known at that time.

H. Schmidt-Böcking
Otto Stern “Physicist, lateral thinker, Nobel Prize winner”

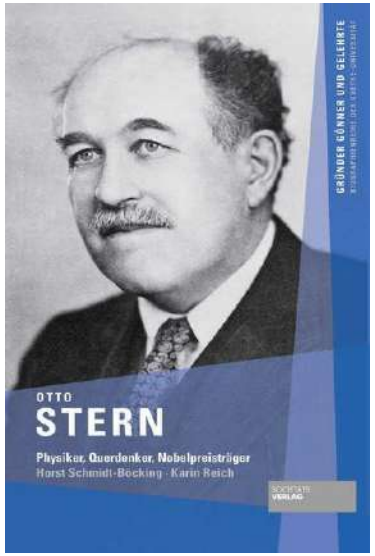

The classical Stern-Gerlach experiment

- **Observation:** spatial splitting of Ag atomic beam in inhomogeneous magnetic field.
- **Classical expectation:** The energy of a magnetic dipole (magnetic moment) would produce a *continuous* energy distribution:

$W = -\vec{\mu} \cdot \vec{B} = \mu B \cos\theta$, with force in inhomogeneous field, given by $\vec{F} = -\vec{\nabla} W$.

Surprisingly, two discrete energy values appeared:

- causing a deflection into an upper and a lower Ag spot.
- Quantum-mechanical dipole behaves completely different from a classical one.

Magnetic moments μ_B and μ_N

In a magnetic field, the energy of the system is proportional to the flux density B:

- Proportionality coefficient: component of m_J in direction of field (“direction of quantization”).
- Unit of measurement is Bohr magneton or nuclear magneton μ_B and μ_N.
- Magnetic moments belong to electronic spin J or nuclear spin I:

$$\mu_J = g_J\mu_B \text{ or } \mu_J = g_I\mu_N$$

Experimental values for Bohr magneton μ_B and nuclear magneton μ_N

Numerical values in terms of $\frac{m}{m_p}$ and $\frac{\mu}{\mu_N}$ available from NIST http://www.nist.gov/pml/data:

$$\mu_B = \frac{e\hbar}{2m_e} = 5.788\,381\,8012\,(26) \times 10^{-5}\ \mathrm{eVT}^{-1}$$

$$\mu_N = \frac{e\hbar}{2m_p} = 3{:}152\,451\,2550\,(15) \times 10^{-8}\ \mathrm{eVT}^{-1}$$

Convention

- For positively charged particles and with $g > 0$ (e.g., protons) : spin and magnetic moment vectors are parallel.
- For negatively charged particles (e.g., electrons) spin and magnetic moment vectors are antiparallel.

Separation of spin states in inhomogenous fields

The energy of a spin state S in a magnetic field B is:

- Numerical values in terms of $\frac{m}{m_p}$ and $\frac{\mu}{\mu_N}$ available from NIST http://www.nist.gov/pml/data:

  Classically: $\mathrm{W} = -\mu B = -\mu \left(\frac{S_z}{S}\right) B$ or

  Quantum-mechanically: $W = g_s \mu_B S \hbar B.$
- System with spin S in magnetic field splits into $2S + 1$ components with magnetic quantum numbers $-S \leq m_S \leq S.$
- In case of hydrogen atoms this is the fine-structure Zeeman effect, as observed in the Stern–Gerlach experiment.
- Forces acting on the spin components in an inhomogeneous magnetic field are different and depend on the sign of m_S.
- Principle of “spin filter” using the spatial separation of spin states.

Sources of polarized atoms (ions)

For practical applications,

- where high beam intensities are desired, Stern-Gerlach arrangement with separation in one dimension is replaced by systems with **rotational symmetries**, i.e., **multipole fields**.
- **Diaphragms** eliminate the wrong components and transmit only the wanted states.
- **Stern-Gerlach filter acts as a nearly perfect polarizer.**

Component with $\boldsymbol{m_J = \pm\frac{1}{2}}$

- of electron spin J of atoms in infinitely strong magnetic field $\sim$ 100 %.
- True as long as particle velocities in beam low enough (e.g., thermal), so that magnets separate two spin components completely.
  - Widths of partial beams small enough to be separable.
  - Widths are a consequence of atoms' velocity distributions and are a function of beam temperature.

Energy levels of the H atom (not to scale!)

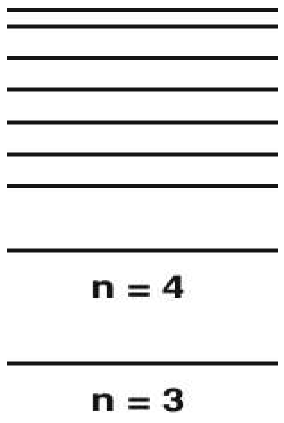

Fine structure: splitting of spectral lines due to electron spin and relativistic correction to Schrödinger Eq.

Lamb shift: interactions between virtual photons from vacuum energy fluctuations and electron moving around hydrogen nucleus in each of these two orbitals.

Hyperfine structure: arises from energy of nuclear magnetic dipole moment interacting with the magnetic field generated by the electrons.

Zeeman effect: splitting of a spectral line into several components in the presence of a static magnetic field.

Rydberg formula

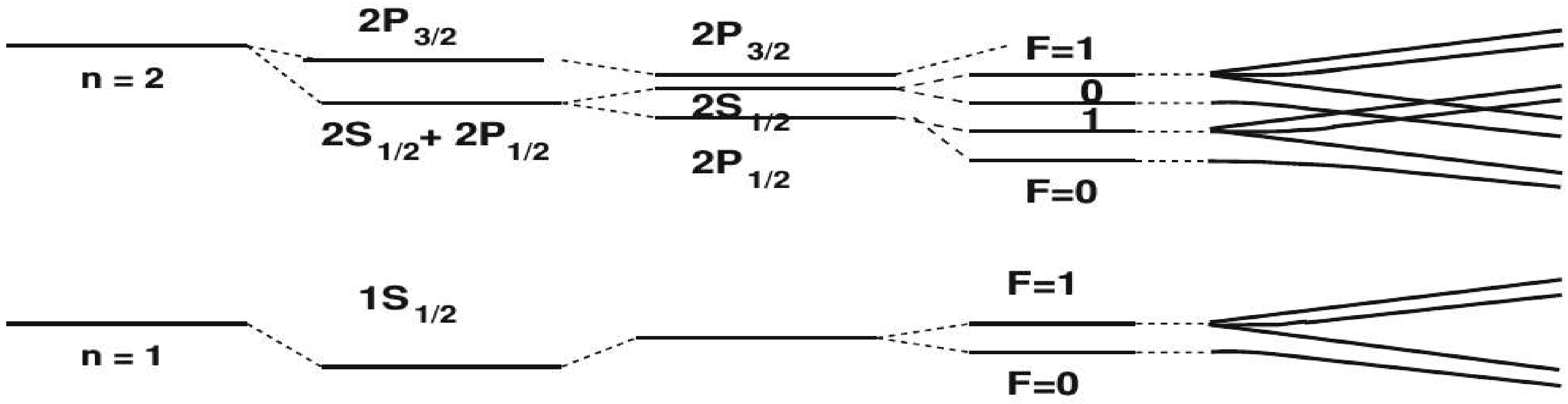

Bohr | Fine Structure | Lambshift | Hyperfine structure | Zeeman effect

Hyperfine Structure (HFS) of hydrogen (deuterium)

The HFS is generated by

- the coupling of the electronic spin $J = \frac{1}{2}$ with nuclear spin $I = \frac{1}{2}$ (hydrogen), or $I = 1$ (deuterium) to the total angular momentum

$$\vec{F} = \vec{I} + \vec{J}, \text{ with state vectors } |F, m_F\rangle.$$

- The eigenvalue equation reads:

$$H_{\text{HFS}} = |F, m_F\rangle = E_F|F, m_F\rangle, \text{ where } H_{\text{HFS}} = a(\vec{I} \cdot \vec{J})$$

- (Here, smaller and different terms such as quadrupole interaction in the Hamiltonian of the HFS were neglected)
- Using $\vec{F}^2 = \hbar^2 F(F+1)$, with

$$\vec{I} \cdot \vec{J} = \frac{1}{2}[F(F+1) - I(I+1) - J(J+1)] \text{ it follows that}$$

$$E_F = \frac{a\hbar^2}{2}\left[F(F+1) - I(I+1) - \frac{3}{4}\right]$$

Thus, the HFS splitting becomes

$$\Delta W = E_{F=I+\frac{1}{2}} - E_{F=I-\frac{1}{2}} = \frac{a\hbar^2}{2} \cdot (2I+1) = \frac{a\hbar^2}{2}\begin{cases} \cdot 3 & \text{for D} \\ \cdot 1 & \text{for H} \end{cases}$$

HFS in magnetic field (Zeeman Effect)

For arbitrary magnetic field, one expands into states with “good” quantum numbers:

- .ie., either in a very weak or very strong magnetic field.
- We are interested in nuclear polarization, so we preferably expand into

$$|I, m_I\rangle|J, m_J\rangle \equiv |m_J, m_I\rangle$$

- Following the rules of vector coupling, we obtain:

$$m_F = m_I + m_J, \text{ and} \left|m_J, m_I\right\rangle = \left|m_J, m_F - m_J\right\rangle,$$

where especially for $m_J \pm \frac{1}{2}$:

$$\left|m_J, m_I\right\rangle = \left|\frac{1}{2}, m_F \pm \frac{1}{2}\right\rangle$$

- The total Hamiltonian reads:

$$H = H_{\text{nuclear}} + H_{\text{electronic}} + (\gamma_I m_I + \gamma_J m_J)B_0 + a\left(\vec{I} \cdot \vec{J}\right) \qquad (+H_{\text{quad.}})$$

Breit-Rabi formula

Solution of Hamiltonian from previous equation

- yields the Breit-Rabi formula

$$E_{F=I\pm\frac{1}{2}} = \frac{\Delta W}{2}\left[\frac{1}{2I+1} - \frac{\gamma_I B m_F}{\Delta W/_2} \pm \sqrt{1 + \frac{4m_F}{2I+1}x + x^2}\right]$$

  With $x = (g_J - g_I)B/\Delta W \approx g_J B \Delta W = \frac{B}{B_{\text{crit}}}$
  - For practical purposes terms with g_I or γ_I are neglected due to the smallness of the nuclear magnetic moment in comparison with the electron magnetic moment.
- Parameter x is (dimensionless) magnetic field, measured in units of magnetic field corresponding to HFS splitting $B_{\text{crit}} = \frac{\Delta W}{(g_J - g_I)\hbar} \approx \frac{\Delta W}{g_J \hbar}$.

⇒ Allows for universal representations of Zeeman effect of HFS which depend only on spin structure.

HFS of the H Atom

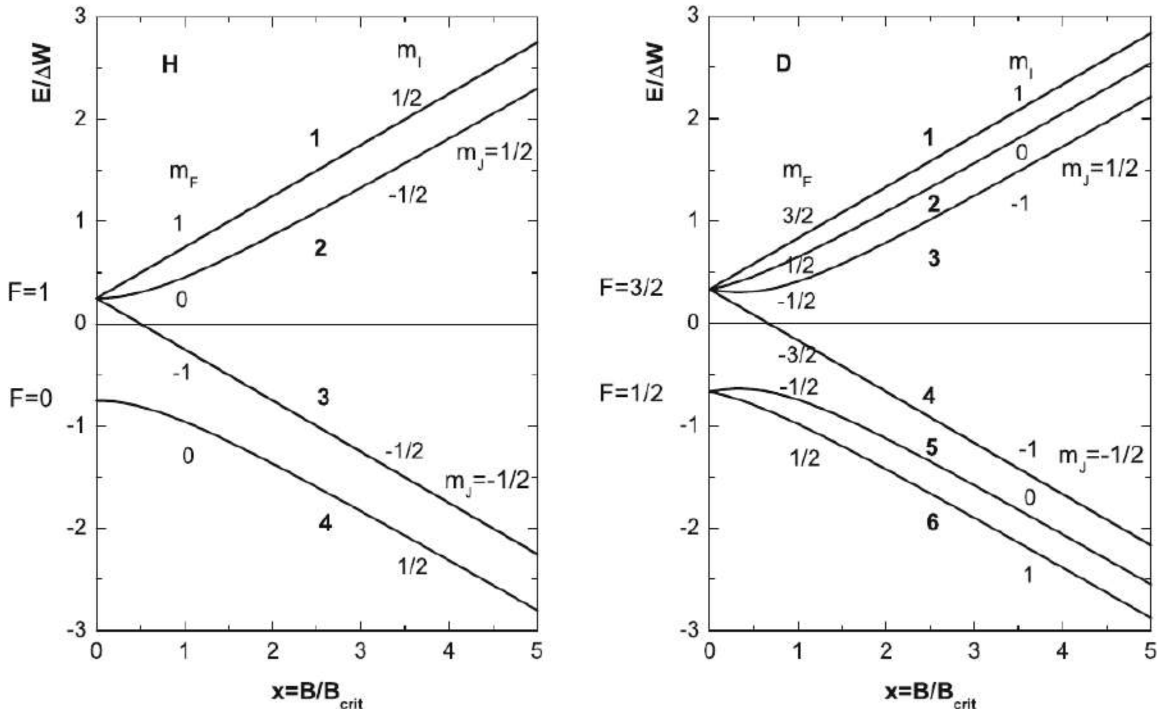

Zeeman splitting (Breit-Rabi diagrams) of the HFS

- As function of magnetic field parameter $x = \frac{B}{B_{\text{crit}}}$ for systems with

$$J = \frac{1}{2}; I = \frac{1}{2} \text{ (e.g., H), and}$$

$$J = \frac{1}{2}; I = 1 \text{ (e.g., D)}$$

- States are numbered consecutively starting with the highest-energy state.

Values of B_{crit} and ΔW for H and D atoms

For the three relevant states (shown on slide 14)

Hydrogen	B_{crit} [mT]	ΔW [MHz]
$\boldsymbol{1S_{\frac{1}{2}}}$	**50.7**	**1420**
$1P_{\frac{1}{2}}$	2.1	60
$2S_{\frac{1}{2}}$	6.4	178

Deuterium	B_{crit} [mT]	ΔW [MHz]
$\boldsymbol{1S_{\frac{1}{2}}}$	**11.7**	**327**
$1P_{\frac{1}{2}}$	0.5	14
$2S_{\frac{1}{2}}$	1.5	41

Calculation of polarization

System with coupled nuclear and electronic spins:

- Calculate polarization of each Zeeman component from the Breit-Rabi formular and take weighted average over all occupied components (slide 17).
- Field dependent occupation numbers of Zeeman states for calculation of polarization are squares of amplitudes of these states.
- Common definitions of polarization:

$$\text{For H:} \quad p^* = \frac{N_+ - N_-}{N_+ + N_-},$$

$$\text{For D:} \quad p^* = \frac{N_+ - N_-}{N_+ + N_0 + N_-}, \quad \text{and} \quad p^*_{zz} = \frac{N_+ + N_- - 2N_0}{N_+ + N_0 + N_-}$$

- Symbol $*$ denotes polarization with respect to quantization axis of states:
  - e.g., magnetic field direction at ionizer.
  - Quantity independent of coordinate system.
  - p^* and p^*_{zz} enter “Figure Of Merit” (FOM) of an experiment.

Nuclear polarization of H, D in weak and strong B fields

	Hydrogen		Deuterium			
	weak B	strong B	weak B		strong B	
state	p^*	p^*	p^*	p^*_{zz}	p^*	p^*_{zz}
1	1	1	1	1	1	1
2	0	-1	$1/3$	-1	0	-2
3	-1	-1	$-1/3$	-1	-1	1
4	0	1	-1	1	-1	1
5			$-2/3$	0	0	-2
6			$-2/3$	0	1	1
$\boldsymbol{m_J = \frac{1}{2}}$	½	0	$1/3$	$-1/3$	0	0

- Last line shows polarization of atoms in all states focused by the system with electron spin $m_J = \frac{1}{2}$:
  - States $|1\rangle + |2\rangle$ for H, and
  - $|1\rangle + |2\rangle + |3\rangle$ for D.

Polarization of Zeeman states of H and D atoms

Polarization of each single Zeeman component of hydrogen and deuterium.

- The hyperfine states are numbered as in the figure on slide 18. Field dependent occupation numbers of Zeeman states for calculation of polarization are squares of amplitudes of these states.
- The polarization of an ensemble of particles (e.g., in a beam), which are in different Zeeman states is obtained by calculating the weighted average of all occupied components.

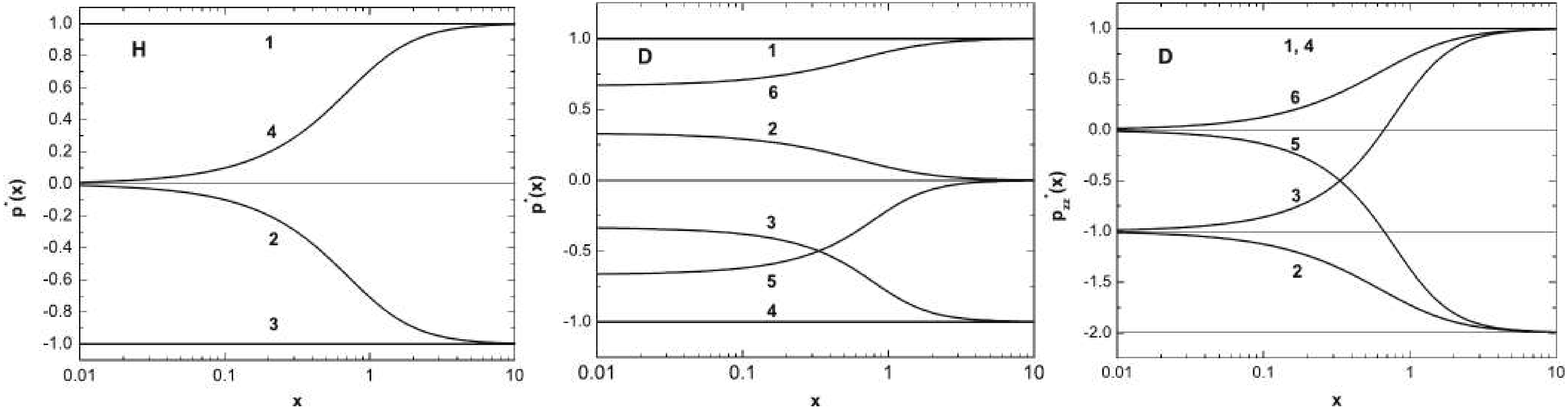

Stern-Gerlach separation of HFS states

In a ground-state atomic beam source:

- Separation strength of HFS states is given by force of inhomogeneous magnetic field acting on the "effective magnetic moment":
    - This is defined as the derivative of the energy $W(B)$, given by Breit-Rabi formula (slide 17), with respect to the field strength B:

$$\vec{F} = -\vec{\nabla} W_{F,m_F} = -\frac{\partial W_{F,m_F}}{\partial B} \vec{\nabla} B = \mu_{\text{eff}} \vec{\nabla} B.$$

- Only for the "pure" components, $\mu_{\text{eff}} = \mu_B$ (see Breit-Rabi diagrams on slide 18), and the separation according to m_J works only for large B fields,

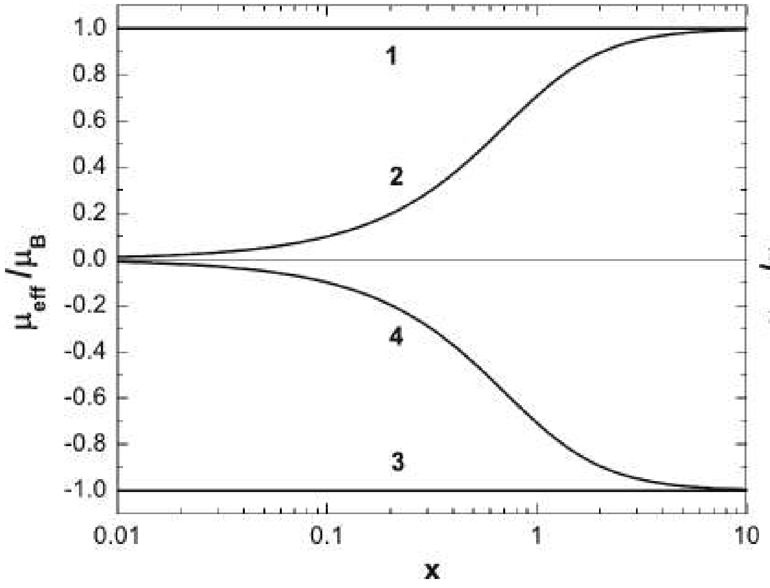

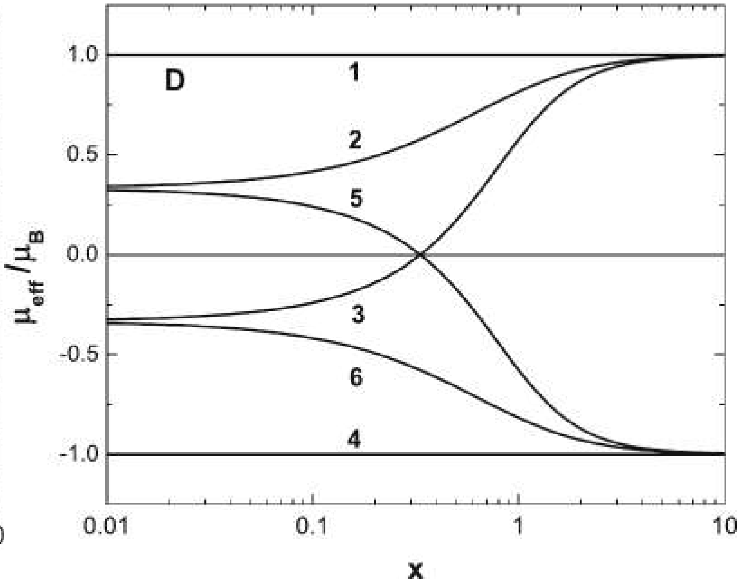

Zeeman separation in multipole magnets

Some comments:

- An efficient separation of Zeeman components uses two-dimensional multipole fields with a **cylindrical symmetry** (quadrupole or sextupole fields).
- The principle of a polarized-ion source for use on accelerators was first formulated by Clausnitzer.
- In sextupole magnets, lens-like focusing action on spin components of atoms possible, whereas other spin components are defocused.

Optics for magnetic moments of neutral atoms to optimize Stern-Gerlach systems

with features like beam transport, phase space, emittance, acceptance, in analogy to charged-particle optics in electric and magnetic fields.

Physics and techniques of atomic beam sources (ABS)

Overview

- Production of H and D ground-state atomic beams,
- Dissociators, beam formation and accomodation,
  - RF discharge dissociators
- State-separation magnets

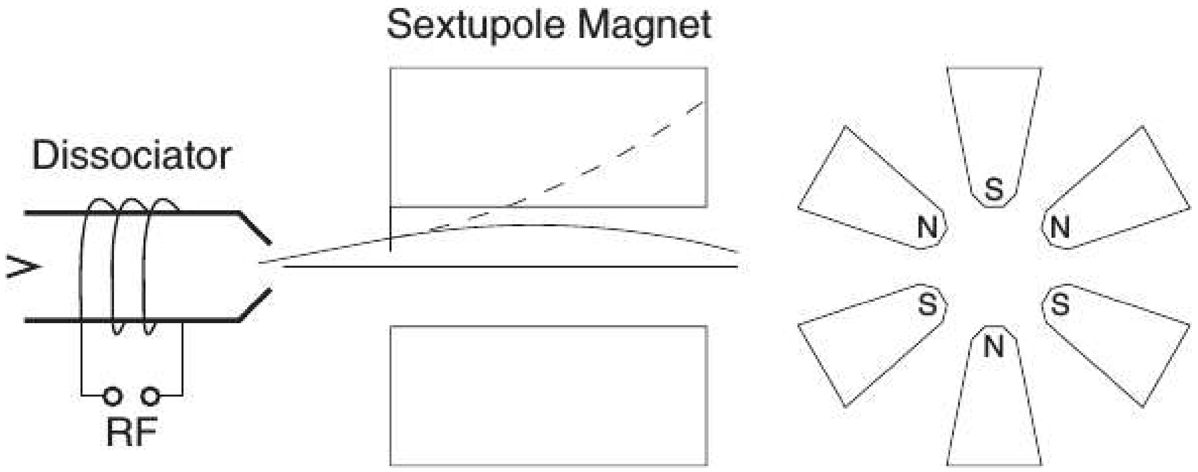

- RF transitions
- Ionizers (not today)
- Polarized (gas) targets and storage cells (not today)

Multipole fields

Historcally, Stern–Gerlach spin-state separation magnet worked only in one dimension:

- Much higher atomic intensities are achieved with rotationally symmetric magnetic fields, i.e., by quadrupole and sextupole magnets acting in two dimensions.
- Permanent magnets as well as electromagnets (including superconducting magnets) are used in sources.
- Nowadays, almost all sources use advantages of modern permanent magnets, so-called “Halbach” magnets.

Quadrupole and sextupole magnets

	Quadrupole	Sextupole
	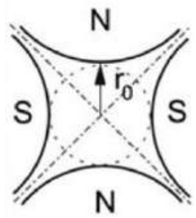	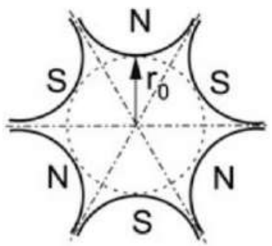
Magnetic potential	$\Phi \sim r^m \cos m\phi$	
Multipole order	$m = 2$	$m = 3$
Magnetic potential	$\Phi \sim r^2 \cos 2\phi$	$\Phi \sim r^3 \cos 3\phi$
Magnetic field (poletip B_0)	$\lvert B(r) \rvert = \left(\frac{B_0}{r_0}\right) r$	$\lvert B(r) \rvert = \left(\frac{B_0}{{r_0}^2}\right) r^2$
Field gradient	$\nabla_r B = \frac{B_0}{r_0}$	$\nabla_r B = \frac{2B_0 r}{{r_0}^2}$
Force	independent of r	Proportional to r
	deflection with constant force	harmonic or hyperbolic trajectories

Permanent magnets before 1980

Multipole magnets

- Originally (i.e., prior to 1980), multipole magnets consisted of separate pole-pieces, formed by permanent magnets with high remanence (such as ALNICO V), ending in angular pole-tips from magnetically soft materials (such as soft iron or Vanadium-Permendur).
- A soft-iron cylinder provided closing of the magnetic circuit. Typical pole-tip fields that could be reached were about 1 T.

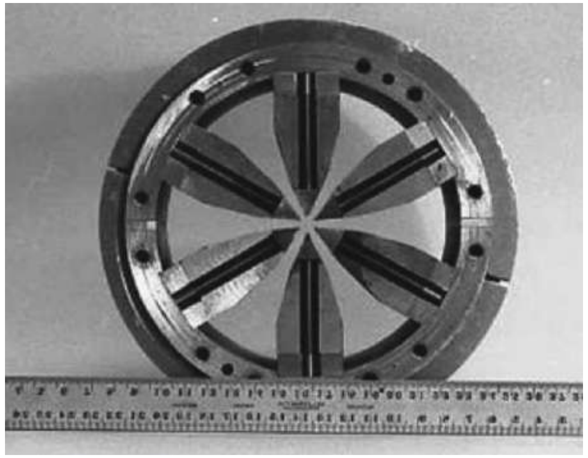

Cross-section of a "classical" permanent sextupole magnet of length 25 cm.

Halbach magnets

New rare-earth magnet material (Nd-Fe-B), developed by Sumitomo Cooperation, Japan:

- The new, stronger magnetic materials can be magnetized in arbitrary direction.
- Using these materials, new designs of multipole magnets emerged with a number of improvements (∼1980).
  - Magnets with smaller surface area and less outgassing were realized.
  - Halbach $2N$-pole magnets: M segments with changing magnetization.
    - after $M/2N$ segments, a pole-piece segment with opposite orientation of magnetization appears.

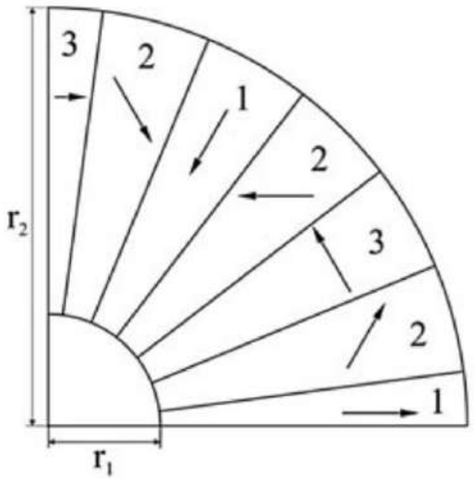

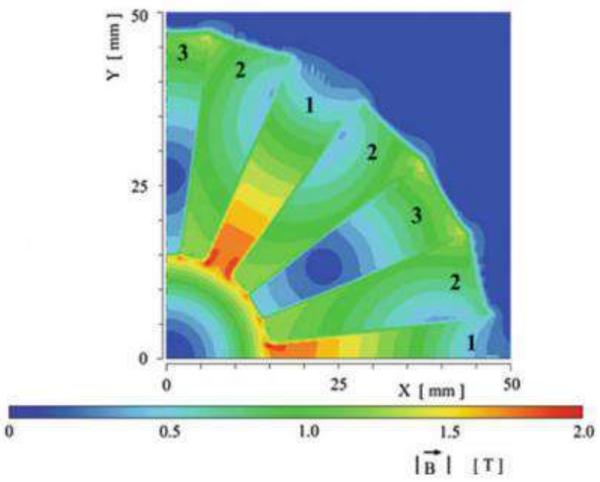

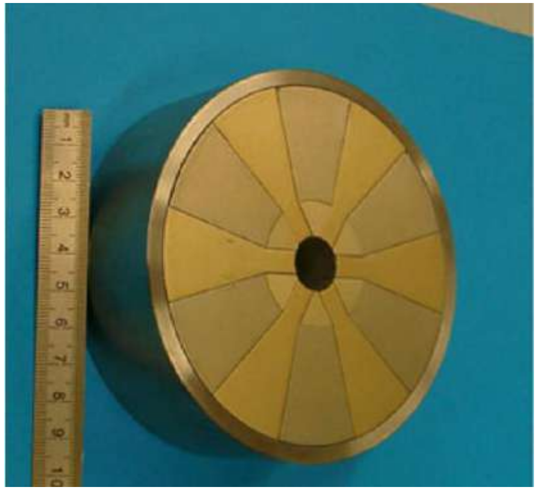

Three different magnetic materials used for ANKE ABS magnets.

System of sextupole magnets

Poletip field B_0^*, inner diameter $\emptyset_0$, outer diameter $\emptyset_1$, magnet length ℓ, and distance Δ from nozzle.

component	B_0^* [T]	$\varnothing_0$ [mm]	$\varnothing_1$ [mm]	ℓ [mm]	Δ [mm]
Nozzle orifice		2.3	3.3		
					15.0
Skimmer		4.4/30.4 [1]		13.0	
					16.9
Diaphragm		9.5/9.9 [1]		2.0	
					3.6
Magnet #1	1.630	10.40/14.12 [1]	39.98	40.01	
					9.4
Magnet #2	1.689	15.98/22.12 [1]	64.04	65.01	
					9.4
Magnet #3	1.628	28.04	94.00	70.01	
					429.7
Magnet #4	1.583	30.04	94.02	38.01	
					101.0
Magnet #5	1.607	30.06	94.00	55.01	
					15.0
Magnet #6	1.611	30.02	94.04	55.00	
					300.0
					337.0
Compr. tube		10.0	11.0	100.0	

[1] Conical opening, first/second number is diameter of entrance/exit (measured).

Presently, permanent magnets provide best way to produce large fields on small diameter.

Designing a magnet system using tracking calculations

Modern polarized atomic beam sources use four to six separated short sextupoles:

- Field strengths and location of magnets determined by tracking calculations, taking into account other requirements:
  - overall space constraints, optimum pumping, insertion of RF transition units, etc.

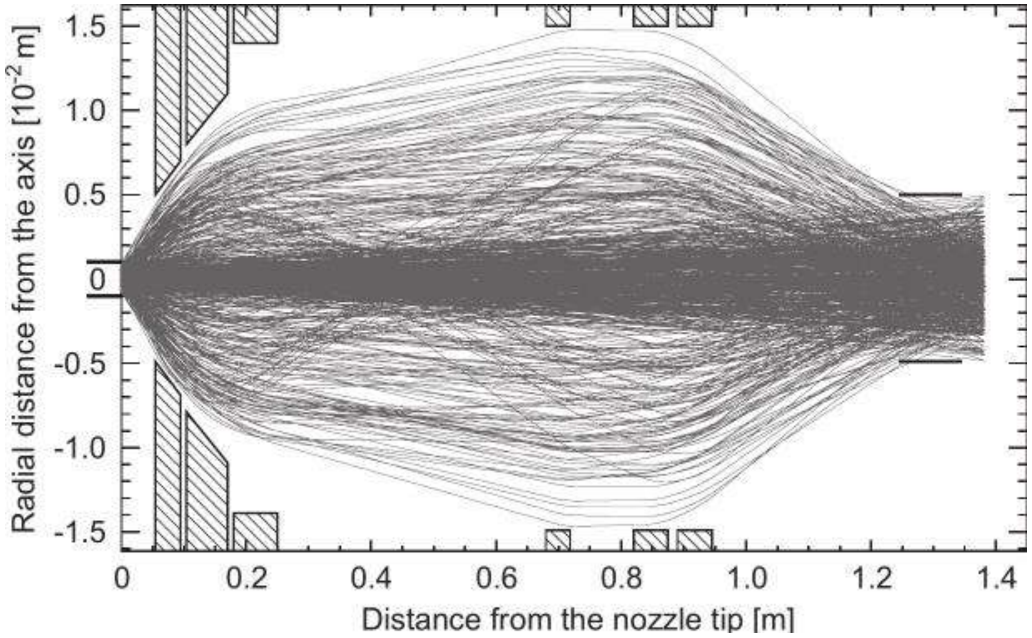

- Projection of 3-dimensional trajectories of hydrogen atoms in hyperfine states $|1\rangle$ and $|2\rangle$:
- Effective magnetic moment $\mu_{\text{eff}} > 0$.

- Trajectories from nozzle ($\emptyset = 2\ \text{mm}, T_{\text{nozzle}} = 60\ K$) to target region:
- Figure reflects magnet system from slide 30, using pole-tip fields of 1.5 T. Positions and radial dimensions of nozzle, apertures of six magnets, and feeding tube are indicated.

RF transitions I

Behind a Stern-Gerlach magnet system, still in a strong magnetic field:

- Atoms are highly polarized with respect to the spin of valence electrons, but nearly unpolarized with respect to nuclear spin, because magnetic field is highly inhomogeneous, i.e., individual polarizations of atoms point in different directions.
- Simply guiding the atoms adiabatically into a region of weak magnetic field, nuclear polarizations of $p^* = \frac{1}{2}$ (H) or $p^* = \frac{1}{3}$ (D) are achieved (see slide 23).

High nuclear polarization requires changing of the occupation of hyperfine states:

- Adiabatic-fast passage method, proposed by Abragam and Winter, induces transitions between different Zeeman hyperfine states.
- This technique is employed in all atomic beam sources targets and provides a high nuclear polarization near the theoretical maximum.
- Due to magnetic field gradients, the RF transitions are independent of the atom velocity.

RF transitions II

Semi-classical picture:

- Beam passes through magnetic field with linear variation of
$$B_0 + \Delta B \rightarrow B_0 - \Delta B$$
- Resonance at B_0 at frequency
$$f = \frac{\mu B}{h}$$
- Spin I with magnetic moment μ_I precesses with angular velocity $\omega = 2\pi f$.

1. Rotating RF field B_1 exerts torque on μ:
2. Spin flips from up to down during passage through gradient field.
3. The rotating field is equivalent to a linear RF field (two counter-rotation fields).

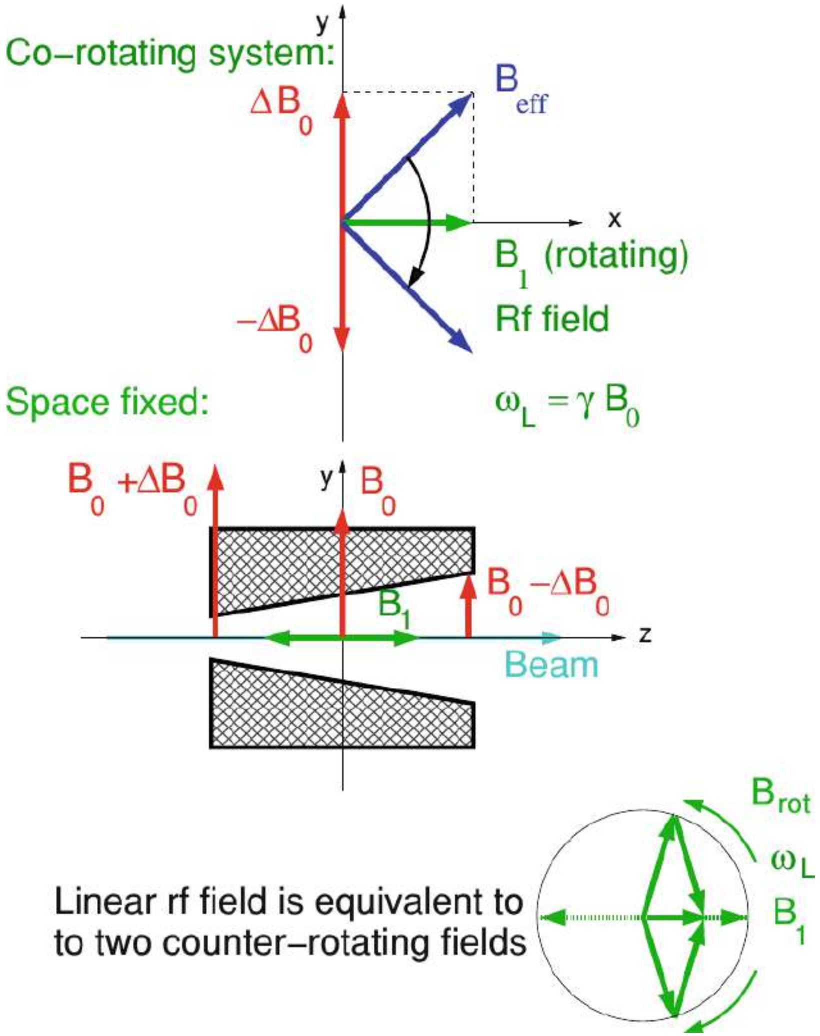

Classification of RF transitions

- RF hyperfine transitions are approximately classified according to the value of the *static* magnetic field B_0 with respect to the critical field B_{crit}:
  - **Weak-field (WFT):** $B_0 \ll B_{\text{crit}}$, transition frequencies typically $5 - 15$ MHz.
  - **Medium-field (MFT):** $B_0 < B_{\text{crit}}$.
  - **Strong-field (SFT):** $B_0 \geq B_{\text{crit}}$, transition frequencies of hundreds MHz to GHz.
- Another classification after Ramsey, refers to change of quantum numbers in transitions:
  - π $(B_1 \perp B_0)$ transitions *within* one F multiplet:
  $$\Delta F = 0, \Delta m_F = \pm 1.$$
  - σ $(B_1 \parallel B_0)$ transitions between *different* F multiplets:
  $$\Delta F = \pm 1, \Delta m_F = 0, \pm 1.$$

RF transition frequencies for H and D

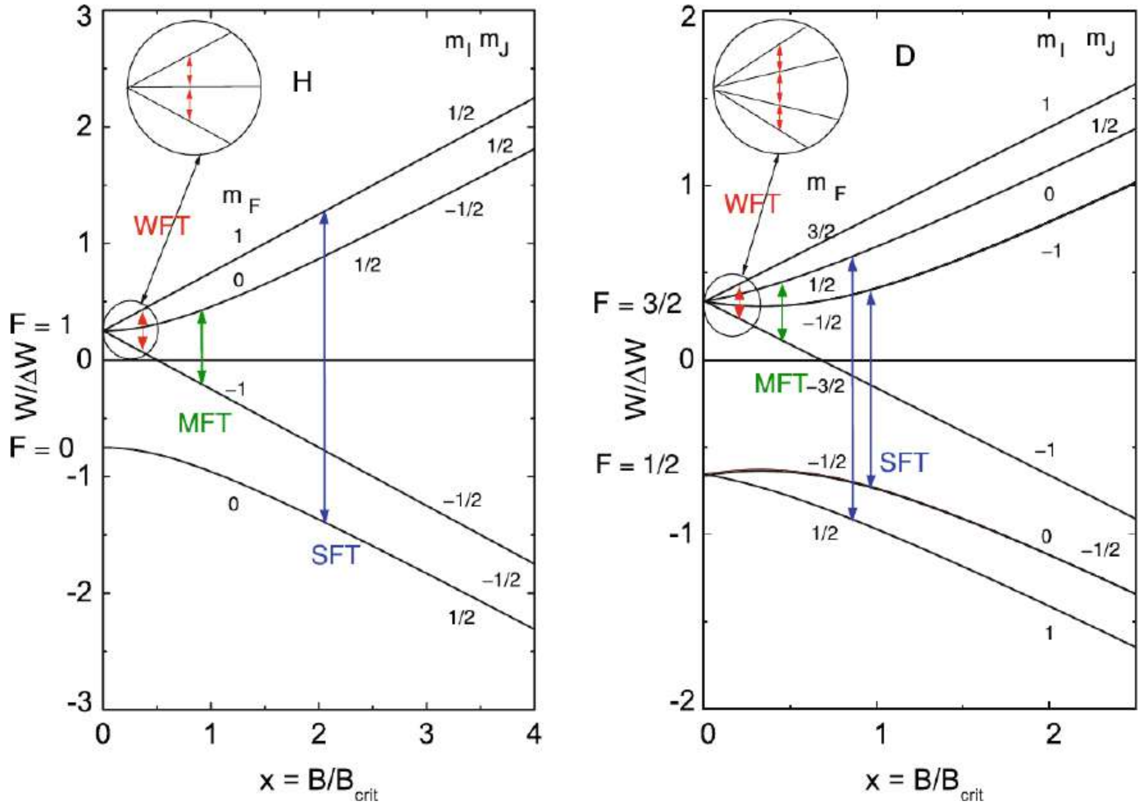

- **WFT** and **MFT**: low-B_0 π transitions.
- **WFT:** in Zeeman region of HFS where m_F states are nearly equidistant ⇒ multi-quantum transitions within F multiplet.
- **MFT:** π transitions at higher B_0 and RF frequencies ⇒ energies of single-photon transitions in one F multiplet sufficiently separated.
- **SFT:** σ or π single-quantum transitions at still higher B_0 between single HFS states.

An Advanced Polarized Proton Source

A. Zelenski et al., J. Phys. Conf. Ser. **295** (2011) 012147

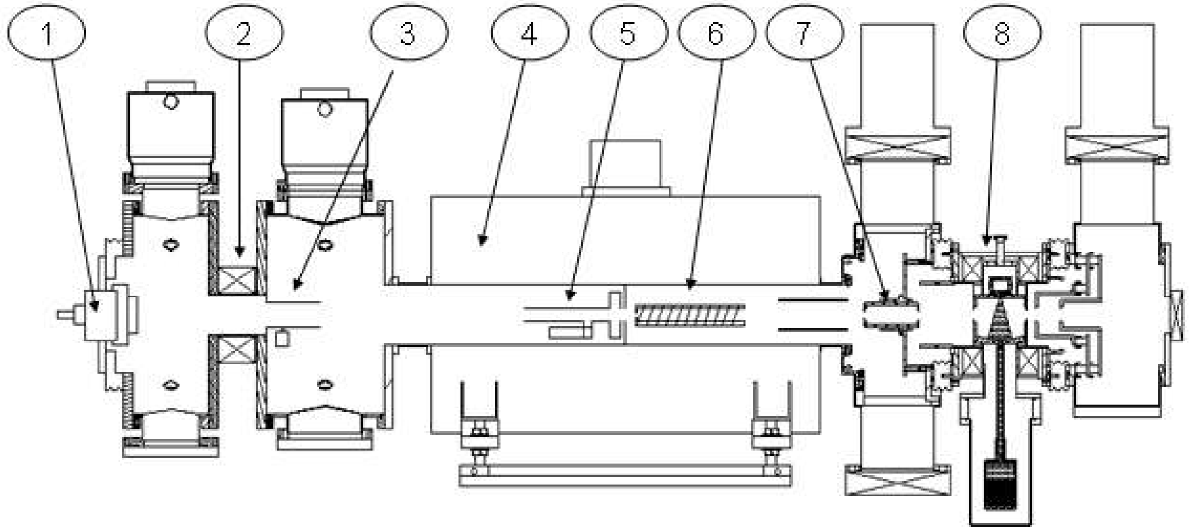

H^+ 10 keV | H^0 10 keV | $H^{0\uparrow}$ 3 keV | $H^{+\uparrow}$ 3 keV | $H^{+\uparrow}$ 35 keV

1. High brightness proton source
2. Focusing solenoid
3. Pulsed hydrogen neutralization cell
4. Superconducting solenoid 30 kG
5. Pulsed He-ionized cell
6. Optically pumped Rb cell
7. Sona shield
8. Sodium-jet ionizer

Optically Pumped Polarized Ion Source at RHIC:

- Current $0.5 - 1.0\ \mathrm{mA}$ in $300\ \mu s$
- Beam polarization $\approx 80\%$ at $35\ \mathrm{keV}$

→ One proton bunch in RHIC

Particle Beam Optics

Lorentz Force:

$$\vec{F} = e(\vec{E} + \vec{v} \times \vec{B})$$

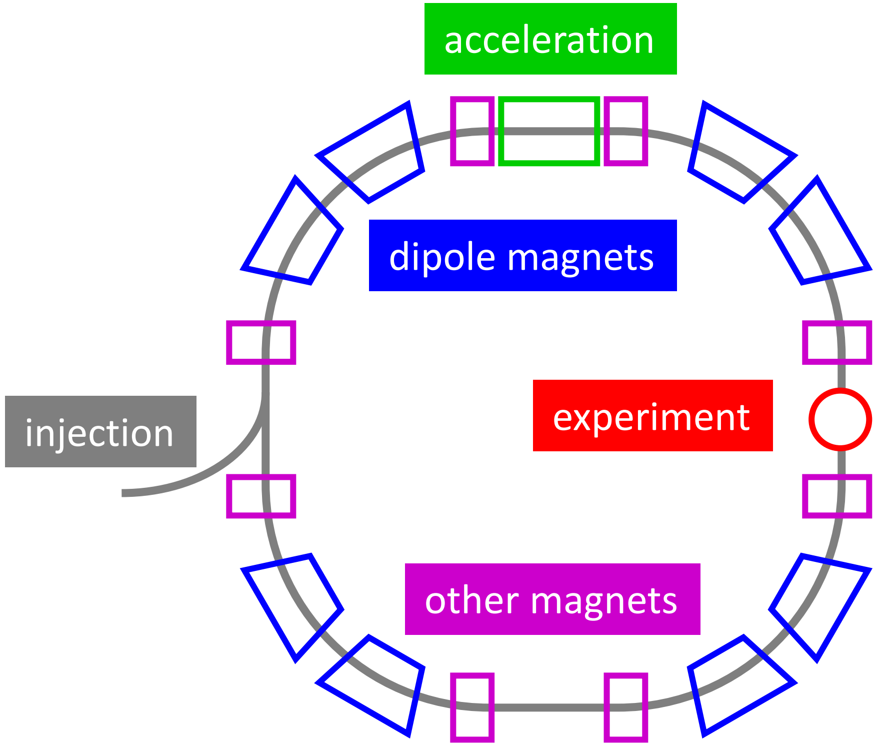

- Lattice to keep the particles on a circle.
- There is a closed orbit.
- Beam has a size and momentum spread.
- Particles oscillate around the closed orbit (betatron oscillation).

F0D0 lattice and orbit envelope

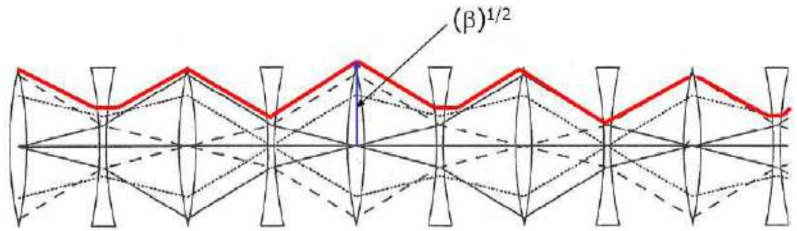

Quadrupole magnets focus in one direction only.

<u>Liouville's theorem:</u> The phase ellipse and the emittance of the beam are invariant.

Particle Beam Optics

Lorentz Force:

$$\vec{F} = e(\vec{E} + \vec{v} \times \vec{B})$$

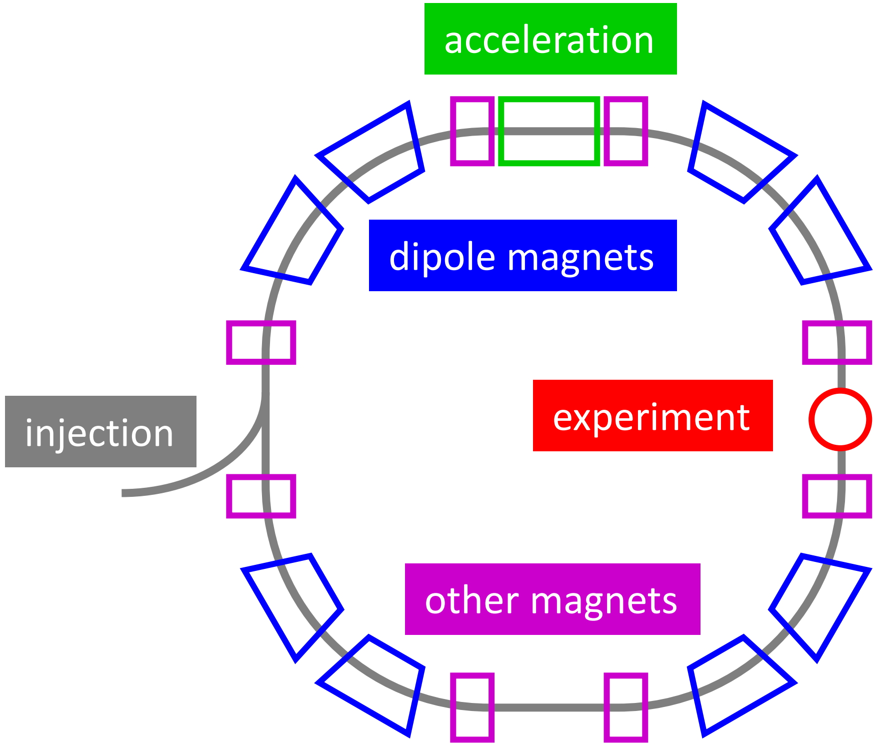

- Lattice to keep the particles on a circle.
- There is a closed orbit.
- Beam has a size and momentum spread.
- Particles oscillate around the closed orbit (betatron oscillation).
- Periodicity can lead to resonances and beam instability

$mQ_x + nQ_z = p$ with (m, n, p) integer numbers

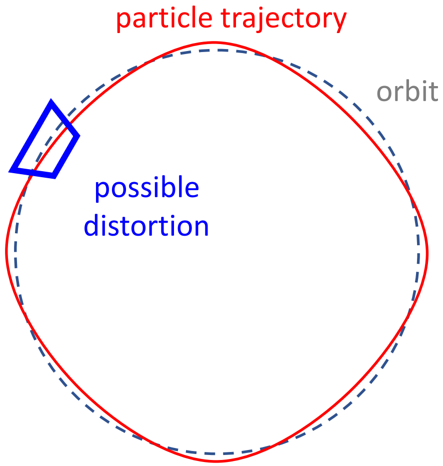

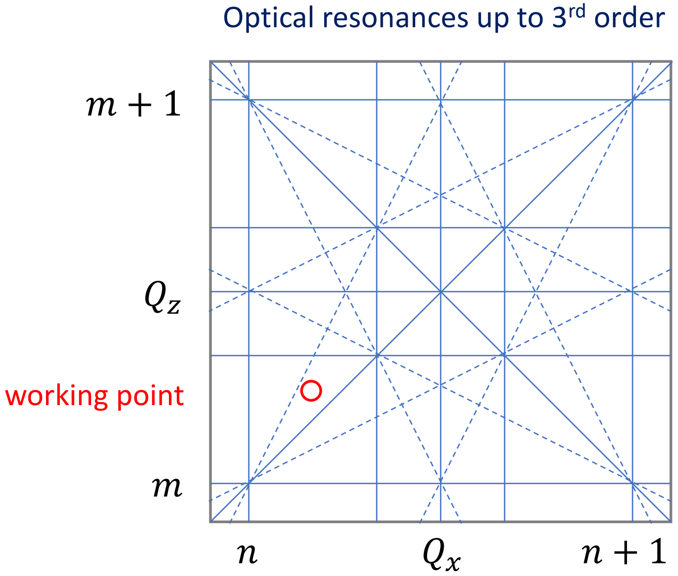

Particle Beam Optics & Spin

Lorentz Force:

$$\vec{F} = e(\vec{E} + \vec{v} \times \vec{B})$$

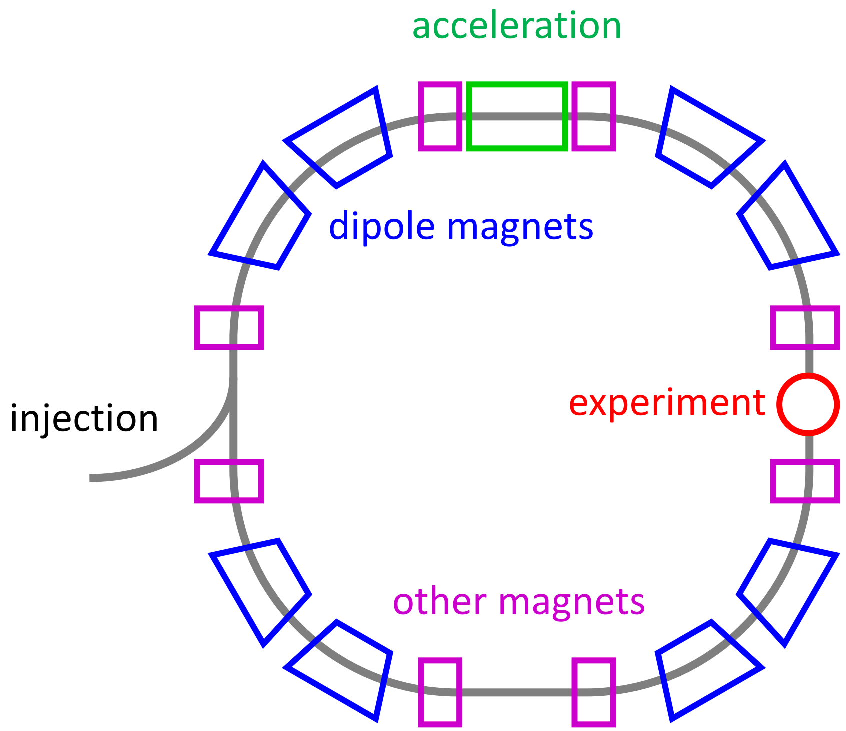

- Lattice to keep the particles on a circle.
- There is a closed orbit.
- Beam has a size and momentum spread.
- Particles oscillate around the closed orbit (betatron oscillation).
- Periodicity can lead to resonances and beam instability.
- The magnetic moment of particles precesses in magnetic fields.

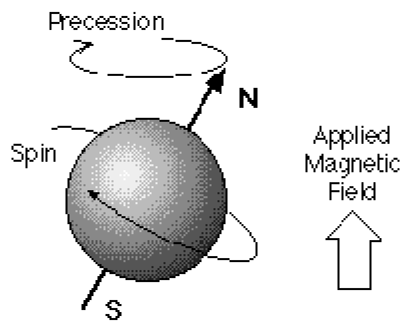

$$\frac{d\vec{S}}{dt} = -\left(\frac{e}{\gamma m}\right)\left[G\gamma\vec{B}_{\perp} + (1+G)\vec{B}_{\parallel}\right] \times \vec{S}$$

$$\frac{d\vec{v}}{dt} = -\left(\frac{e}{\gamma m}\right)\vec{B} \times \vec{v}$$

Proton $\mathrm{G} = 1.7928$

$$\gamma = E/m$$

Depolarizing Resonances

Thomas-BMT equation:

$$\frac{d\vec{S}}{dt} = -\left(\frac{e}{\gamma m}\right)\left[G\gamma\vec{B}_{\perp} + (1+G)\vec{B}_{\parallel}\right] \times \vec{S}$$

$$\frac{d\vec{v}}{dt} = -\left(\frac{e}{\gamma m}\right)\vec{B} \times \vec{v}$$

Proton $\mathrm{G} = 1.7928$

$\gamma = E/m$

L.H. Thomas "The kinematics of an electron with an axis." *The London, Edinburgh, and Dublin Philosophical Magazine and Journal of Science* 3.13 (1927)

V. Bargmann, L. Michel, and V.L. Telegdi "Precession of the polarization of particles moving in a homogeneous electromagnetic field." *Physical Review Letters* 2.10 (1959)

- Spin tune Q_s is the number of precessions per revolution.
- Two types of depolarizing resonances
  - Intrinsic resonances

    $$\gamma G = kP \pm (\nu_y - 2)$$

  - Imperfection resonances

    $$\gamma G = k$$

Resonance strength depends on the local orbit distortion, magnetic field, and crossing speed.

Number of resonances grows linearly with the top energy.

Example: COSY

Cooler Synchrotron at FZ Jülich, Germany

Proton accelerator / storage ring

$p_{max} = 3.3$ GeV/c

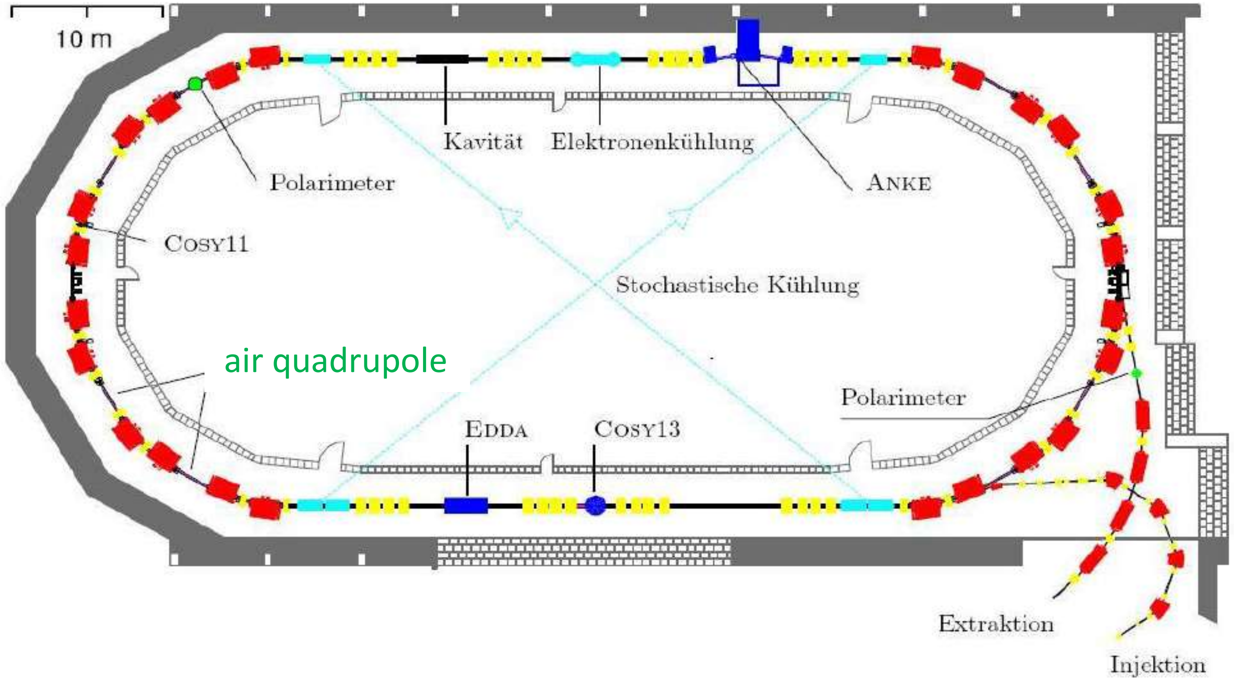

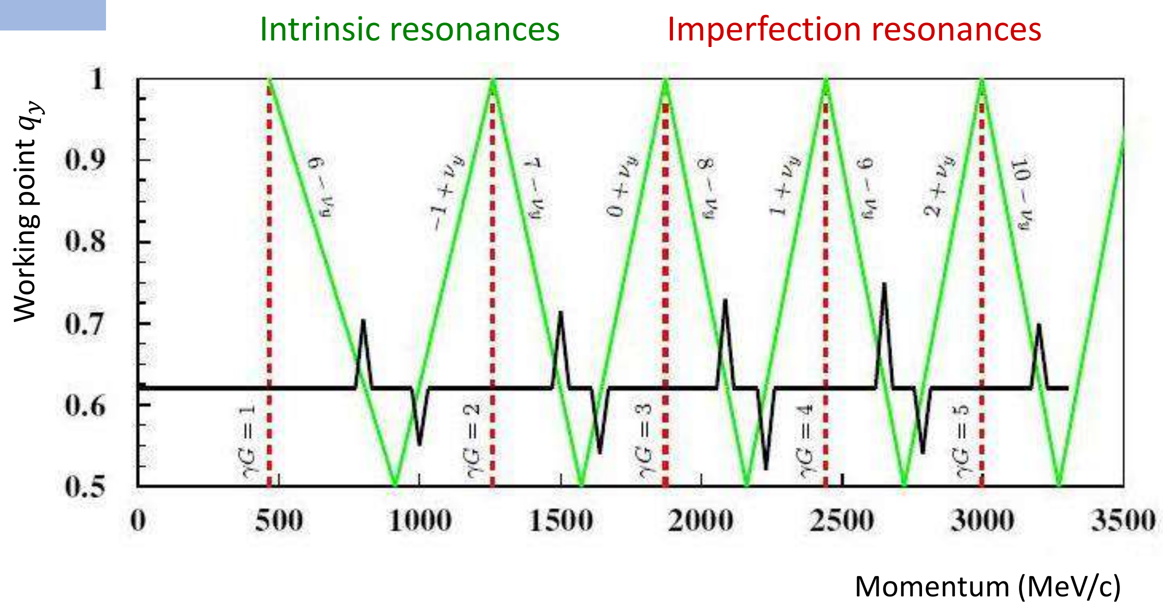

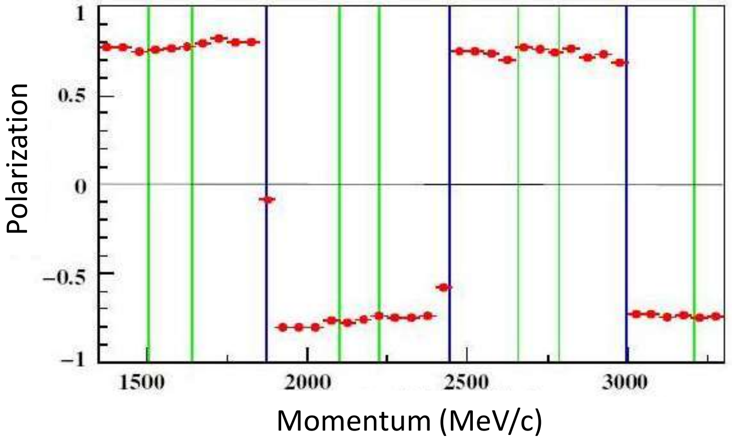

The Relativistic Heavy Ion Collider

“Configuration Manual Polarized Proton Collider at RHIC.” I. Alekseev et al. (2004)

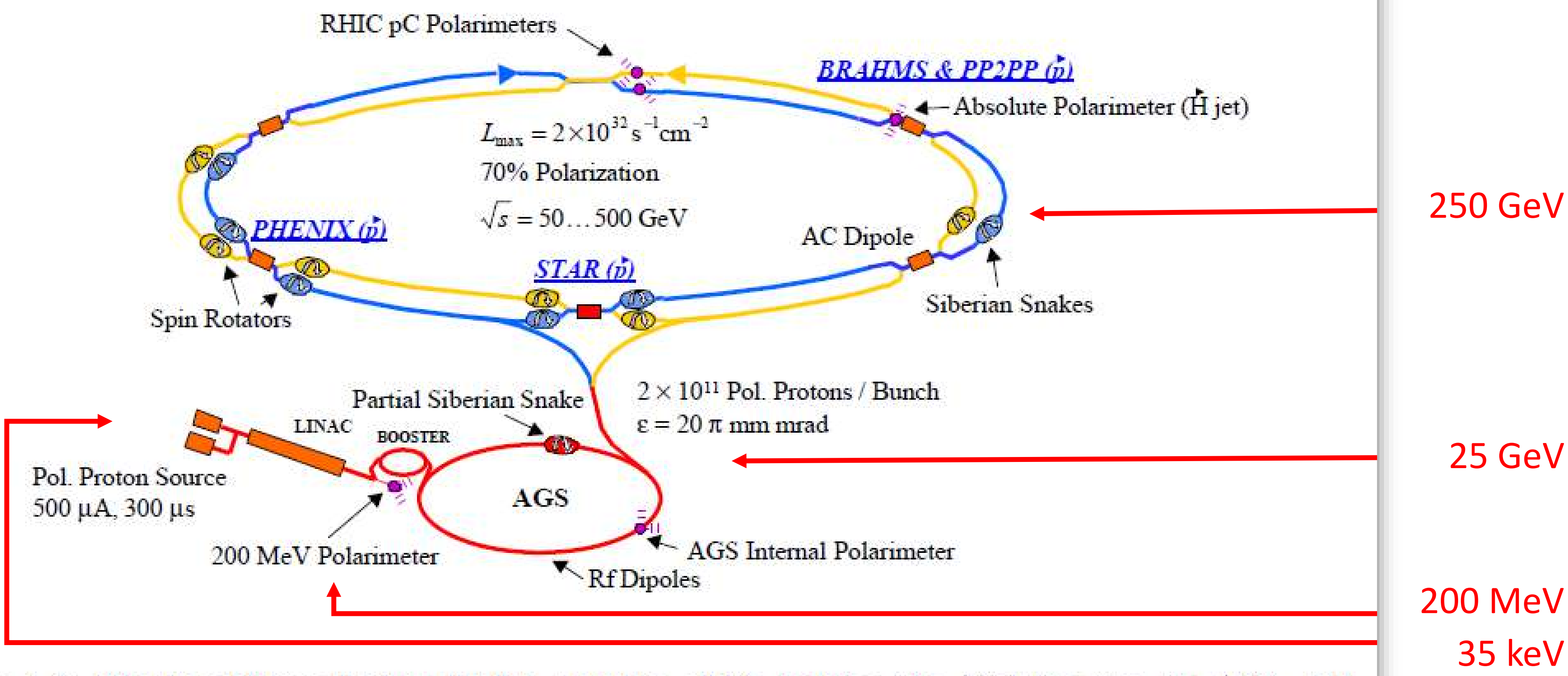

Figure 1.1: The Brookhaven hadron facility complex, which includes the AGS Booster, the AGS, and RHIC. The RHIC spin project will install two snakes per ring with four spin rotators per detector for achieving helicity-spin experiments.

Spin Resonances in RHIC

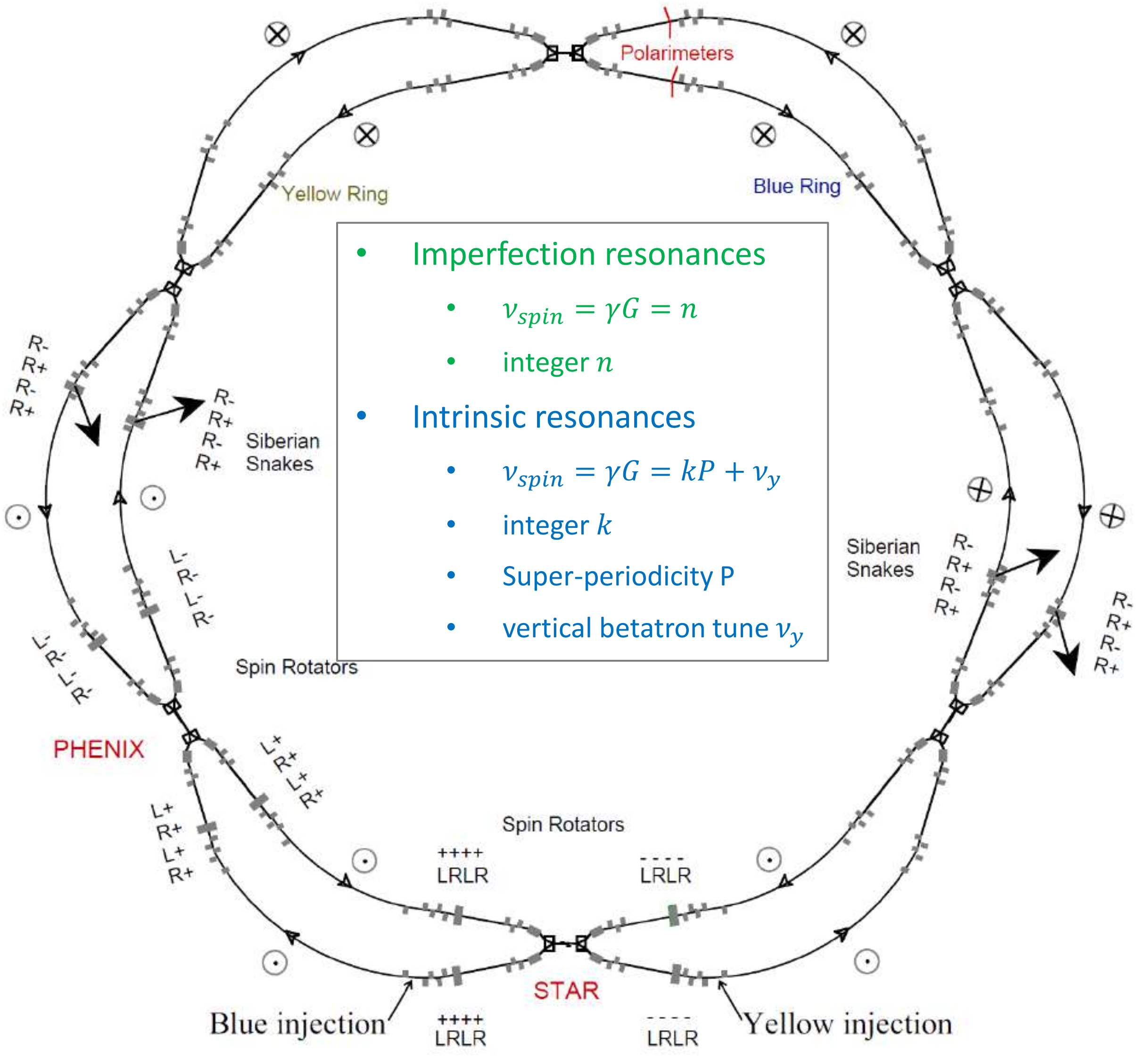

- Imperfection resonances
  - $\nu_{spin} = \gamma G = n$
  - integer n
- Intrinsic resonances
  - $\nu_{spin} = \gamma G = kP + \nu_y$
  - integer k
  - Super-periodicity P
  - vertical betatron tune ν_y

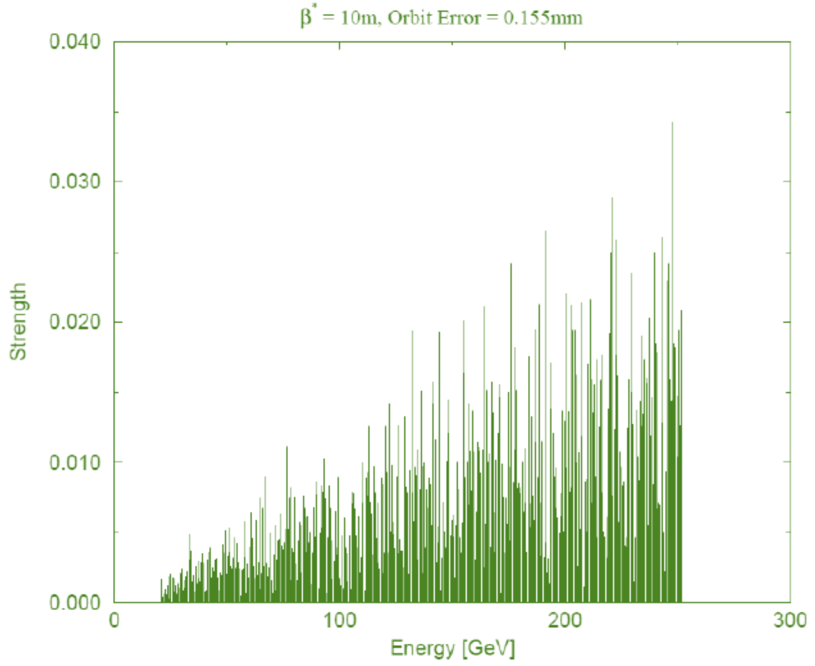

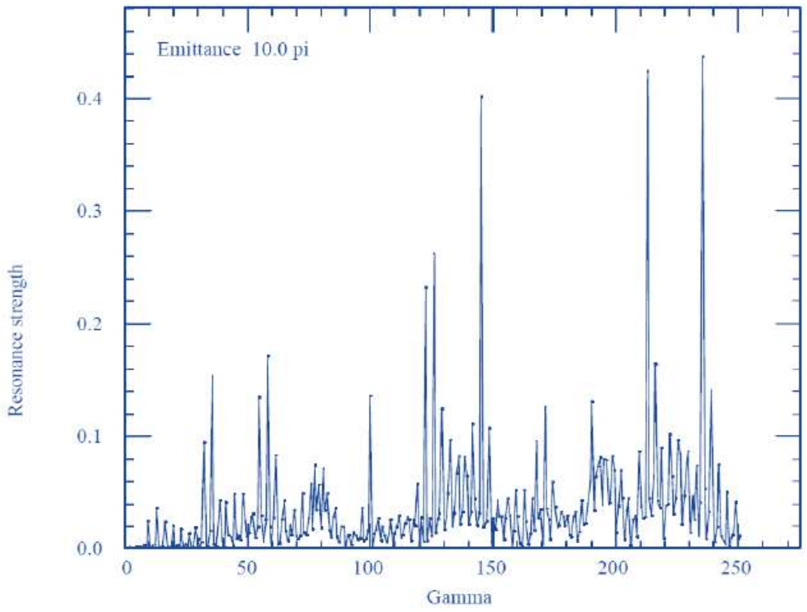

Resonance Mitigation

- Deliberately advance the spin precession to avoid resonance conditions
- Group of dipole magnets with alternating horizontal and vertical field directions which rotates the spin vector by 180°
- **Siberian Snakes:** Ya. S. Derbenev, A.M. Kondratenko "Polarization kinematics of particles in storage rings." Sov. Phys. JETP 37 (1973)

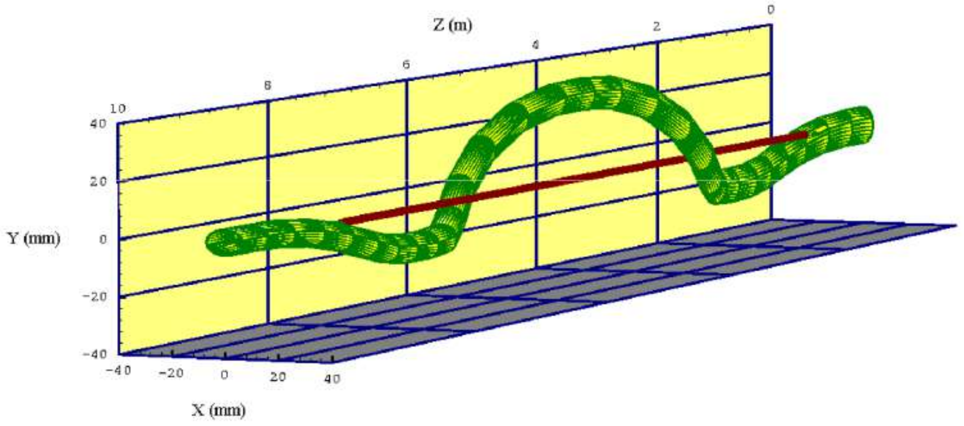

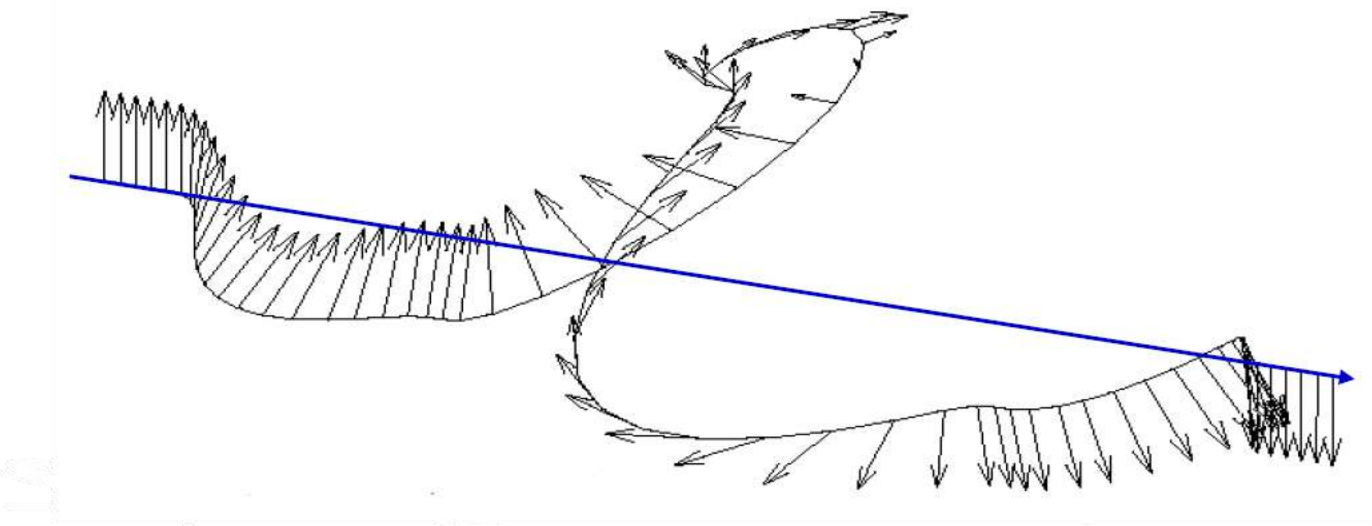

Spin Motion through Siberian Snake

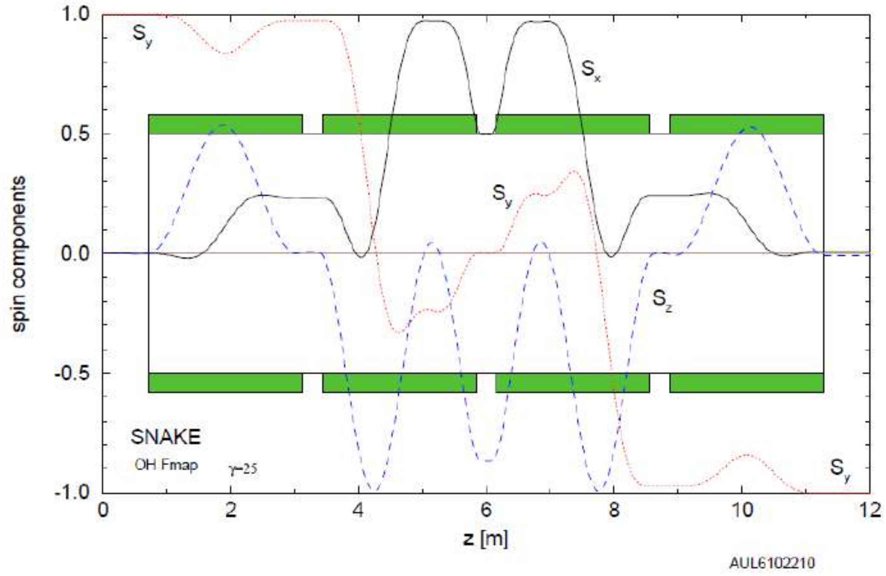

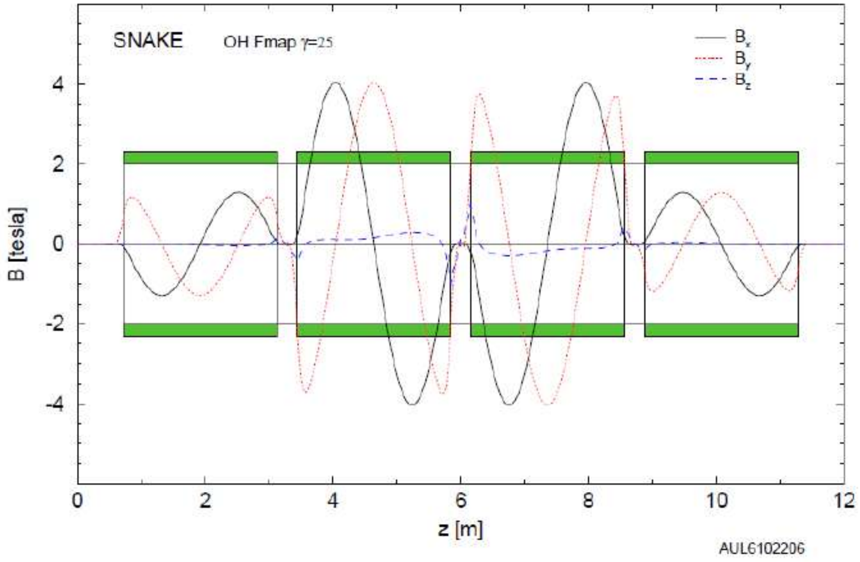

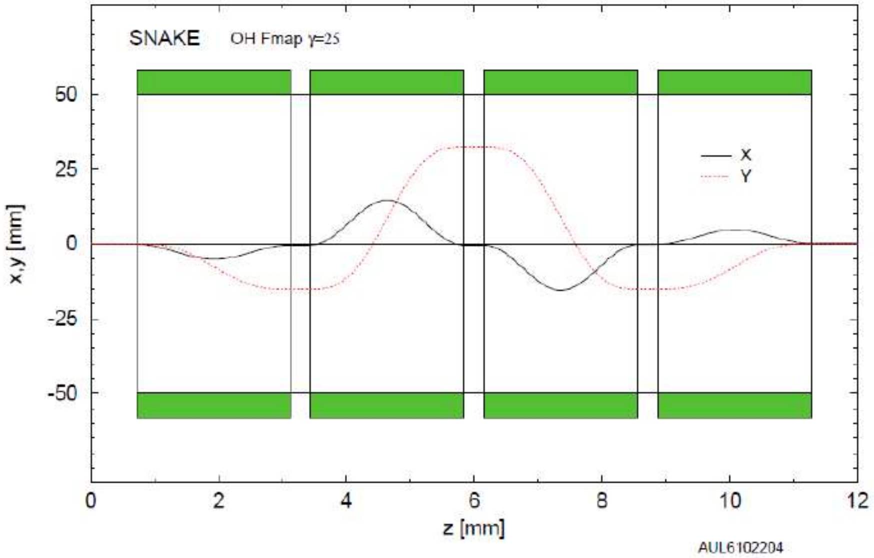

RHIC Proton Polarization

During the first 250 GeV beam operation in 2009

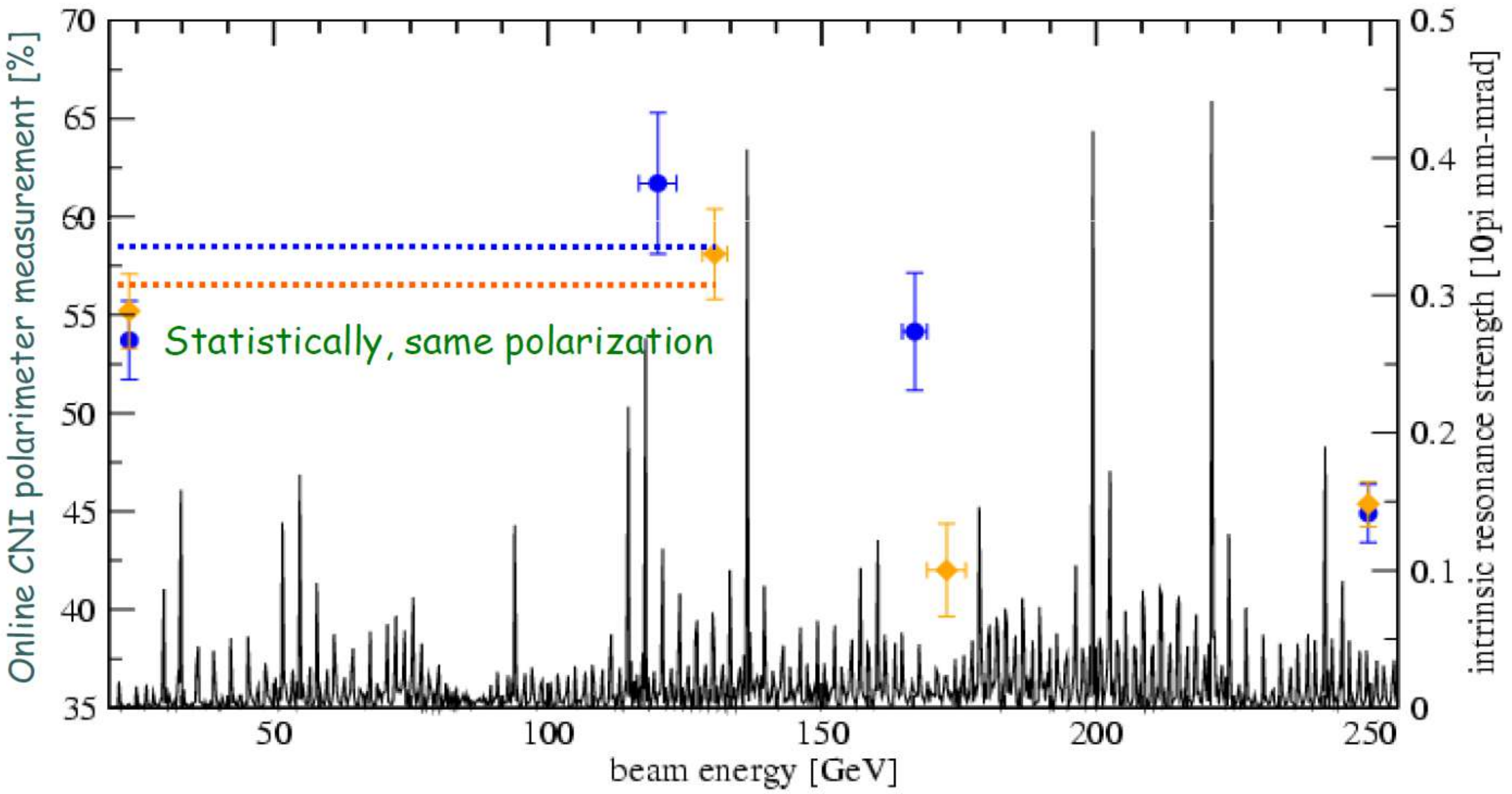

Spin Motion through a Spin Rotator

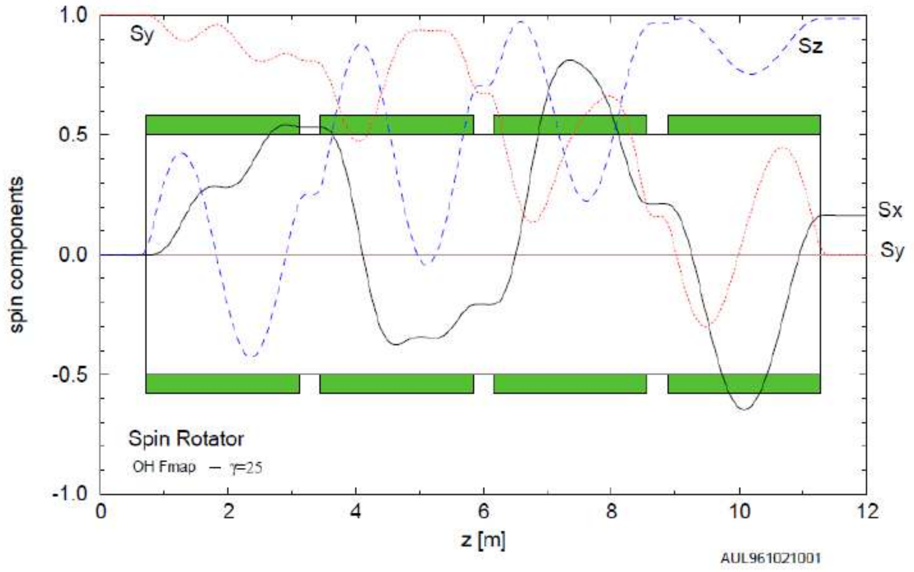

- Stable spin direction in a circular accelerator is vertical.
- Experiments also require longitudinal polarization.
- Spin rotators before and after each experiment.
- Transverse polarization remnant can cause systematic uncertainties in physics observables.

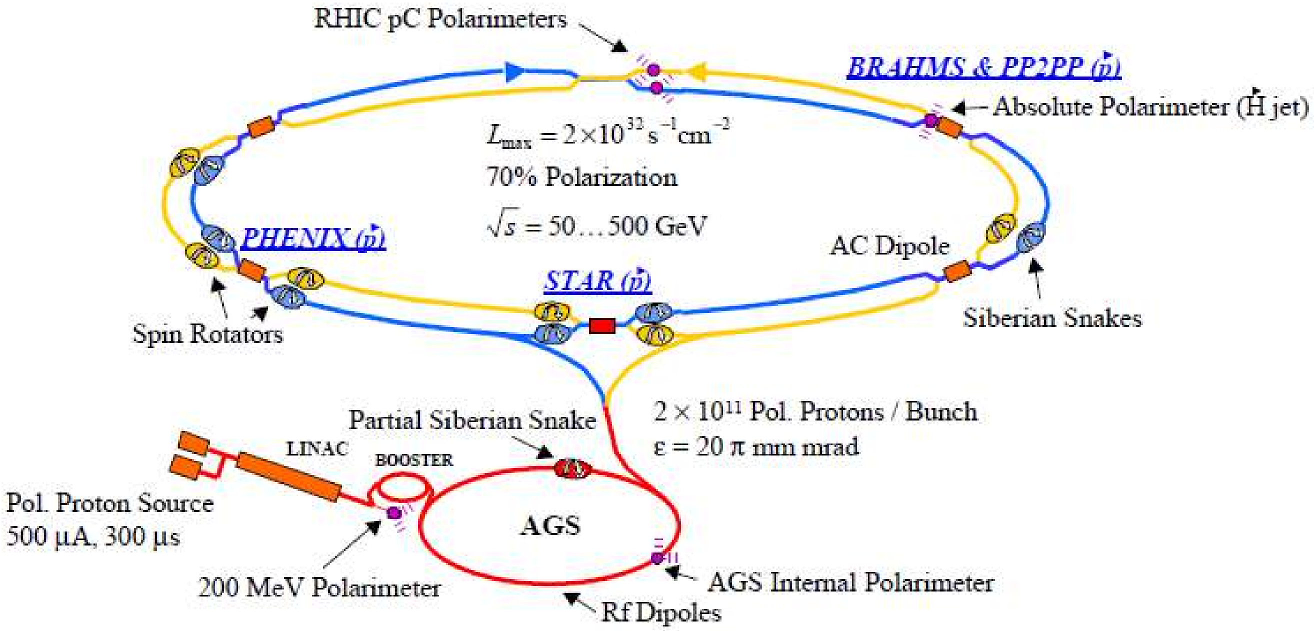

Polarized Beams at EIC

- **Proton beam polarization has to be measured between $50 - 275$ GeV.**
- Electron beam polarization has to be measured between $5 - 18$ GeV.
- Each store may be 8 hours long. Possibly shorter?
- The beams are bunched and will have alternating polarization states to reduce time-dependent systematic uncertainties.
- Bunch spacing is around 10 ns (close to 1300 bunches in each ring).

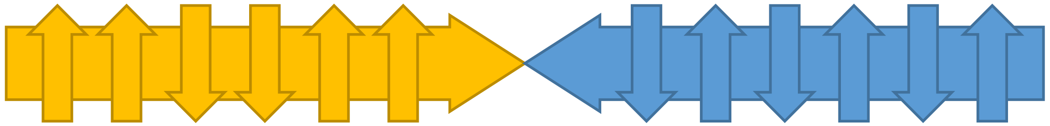

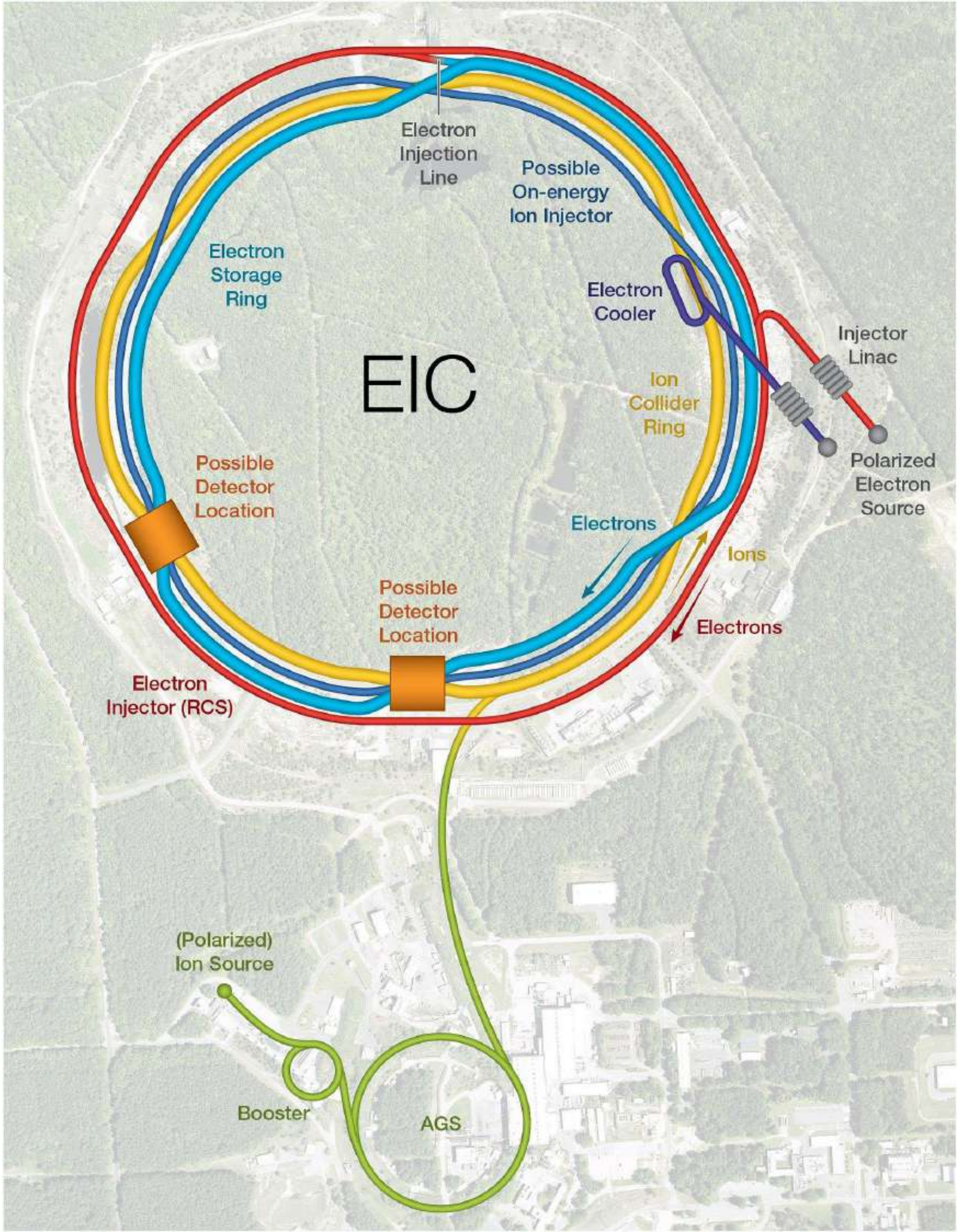

Requirements for Polarimetry

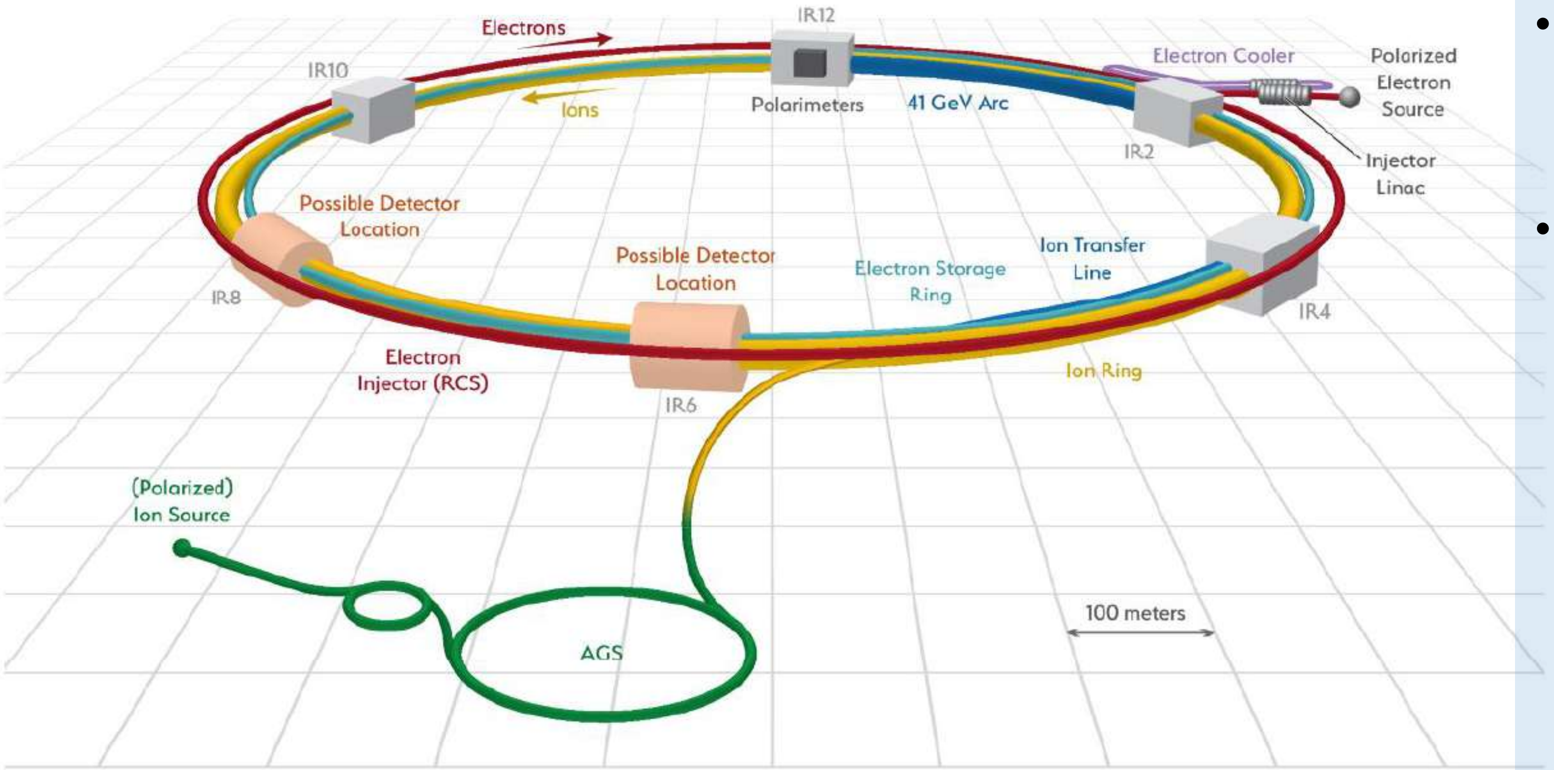

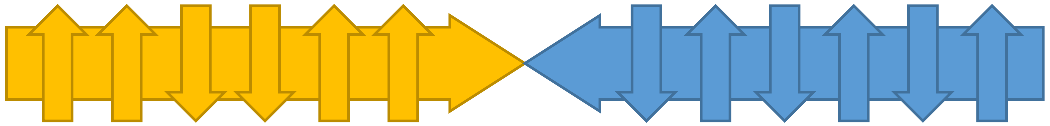

- Required:
  - **Absolute beam polarization**
    $\Delta P/P \approx 1\%$
- Consider:
  - Time-dependence (polarization decay)
  - Bunch-by-bunch polarization
  - Polarization profile of bunches
  - Polarization during ramp (acceleration)
  - Polarization vector at experiment
  - Physics program includes options beyond $\vec{p}$ (spin $\frac{1}{2}$):
    - $\vec{d}$ (spin 1) and $^3\overrightarrow{\mathrm{He}}^{++}$ (spin $\frac{1}{2}$)

3. Polarimetry of High Energy Hadron Beams

Polarization of Particle Bunches

A bunch of particles in vacuum travelling at almost the speed of light

Goes in circles, will be back in about $13\ \mu\mathrm{s}$ $(78\ \mathrm{kHz})$.

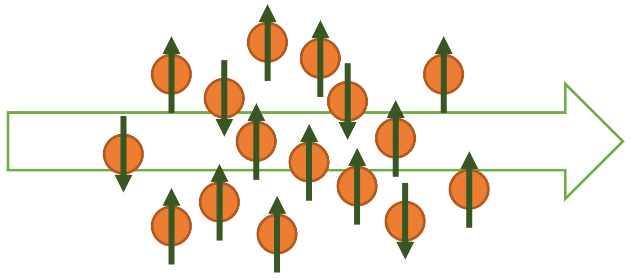

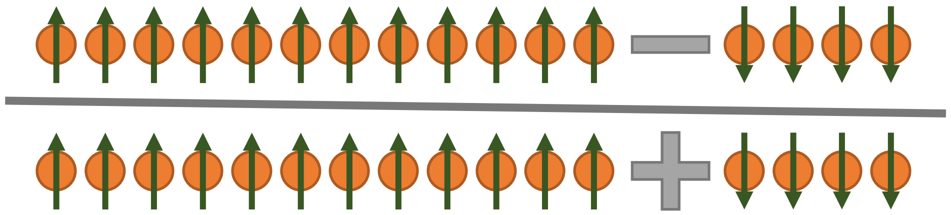

- For the determination of the polarization, we will have to devise an experiment which is spin-dependent.
- Need a representative sample of scattered particles to make conclusive statements about the polarization.
- Only a fraction of the scattering probability will depend on the spin: $\sigma^{\uparrow\downarrow} = \sigma_0 \pm \sigma_s = \sigma_0(1 \pm a_s)$
- It is convenient to introduce an asymmetry: $\epsilon = (\sigma^{\uparrow} - \sigma^{\downarrow})/(\sigma^{\uparrow} + \sigma^{\downarrow}) = a_s$

The Right Frame

- Momentum and spin direction define a coordinate system.

  Longitudinal $\boldsymbol{L}$

  Normal $\boldsymbol{N}$

  Sideways $\boldsymbol{S}$

$$\boldsymbol{S} = \boldsymbol{N} \times \boldsymbol{L}$$

$$\boxed{\varepsilon = A_N \cdot P = \frac{N_L - N_R}{N_L + N_R}}$$

refers to the projectile

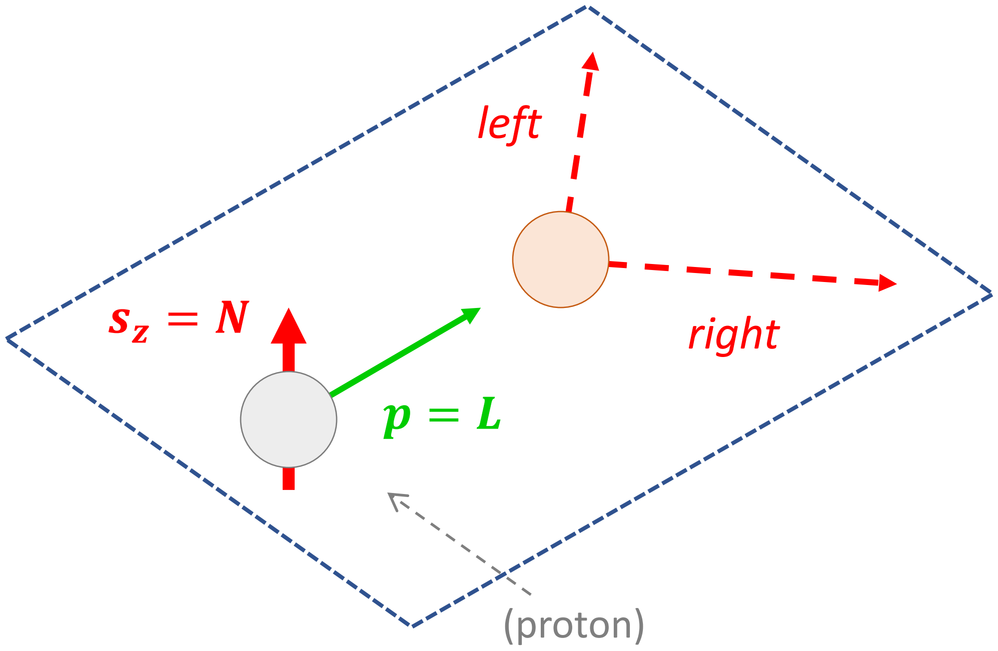

Analyzing power A_N

Polarization $P = \frac{n^{\uparrow} - n^{\downarrow}}{n^{\uparrow} + n^{\downarrow}}$

Transverse Single-Spin Asymmetries

- Elastic scattering obeys parity conservation and time invariance.
- Collision is symmetric (in the center-of-mass frame), recoil and ejectile are indistinguishable.

$$\frac{d\sigma}{\mathrm{d}\Omega} = \frac{d\sigma}{d\Omega_0}\left(1 + P_{beam}A_{00N0} + P_{target}A_{000N}\right)$$

ejectile, recoil, projectile, target

- For elastic scattering:

$$\boxed{A_{00N0} = A_{000N}}$$

$$P_{Beam} = \frac{\varepsilon_{Beam}}{\varepsilon_{Target}} P_{Target}$$

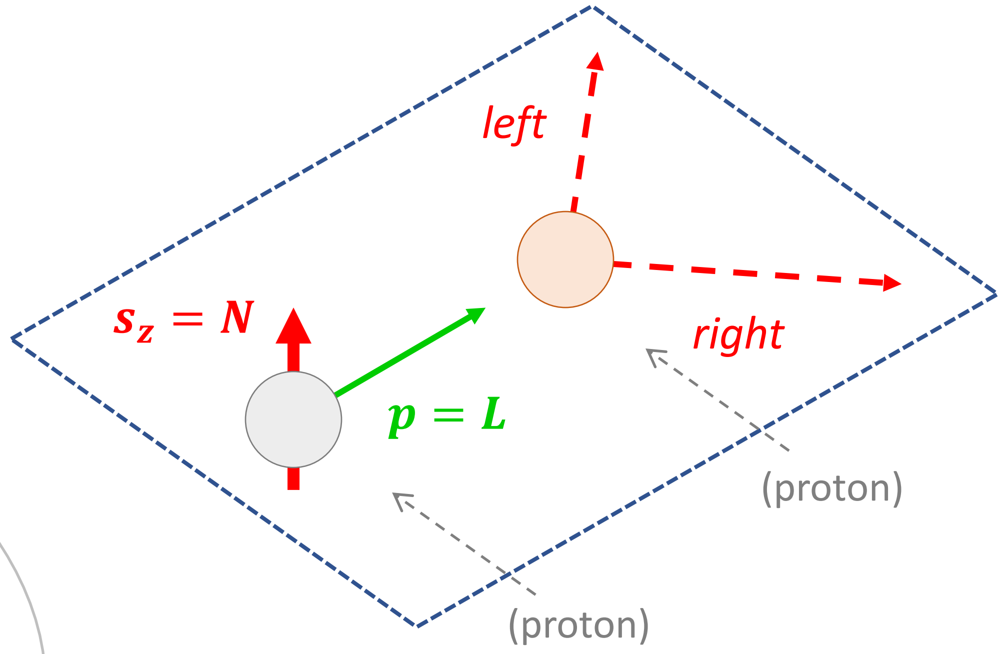

Remember, we just call this A_N

Elastic Scattering at RHIC energies

- Beam momentum is $100 - 250\ \mathrm{GeV}$.
- Significant analyzing power exists in the **Coulomb-Nuclear Interference region**.

$$\varphi(s,t) = \langle \lambda_C \lambda_D | \varphi | \lambda_A \lambda_B \rangle$$

$$\varphi_1(s,t) = \left\langle +\frac{1}{2} + \frac{1}{2} |\varphi| + \frac{1}{2} + \frac{1}{2} \right\rangle$$

$$\varphi_2(s,t) = \left\langle +\frac{1}{2} + \frac{1}{2} |\varphi| - \frac{1}{2} - \frac{1}{2} \right\rangle$$

$$\varphi_3(s,t) = \left\langle +\frac{1}{2} - \frac{1}{2} |\varphi| + \frac{1}{2} - \frac{1}{2} \right\rangle$$

$$\varphi_4(s,t) = \left\langle +\frac{1}{2} - \frac{1}{2} |\varphi| - \frac{1}{2} + \frac{1}{2} \right\rangle$$

$$\varphi_5(s,t) = \left\langle +\frac{1}{2} + \frac{1}{2} |\varphi| + \frac{1}{2} - \frac{1}{2} \right\rangle$$

A. Poblaguev et al., Phys. Rev. D 79, 094014 (2009)

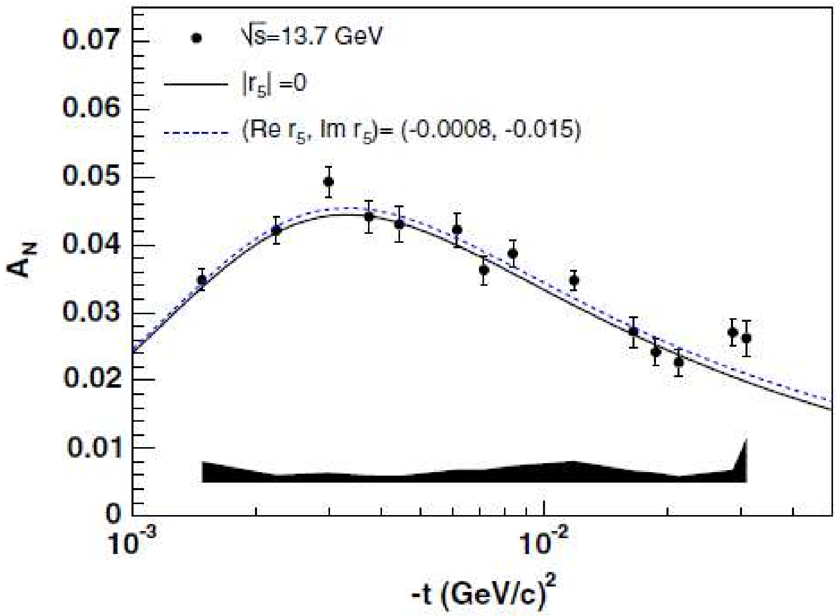

$$A_N \frac{ds}{dt} = -\frac{4\pi}{s^2} \mathrm{Im}\left[\varphi_5^{em*}(s,t)\varphi_+^{had}(s,t) + \varphi_5^{had*}(s,t)\varphi_+^{em}(s,t)\right]$$

no-flip amplitude: $\varphi_+(s,t) = \frac{1}{2}[\varphi_1(s,t) + \varphi_3(s,t)]$

Elastic Scattering at RHIC energies

- Beam momentum is $100 - 250\ \mathrm{GeV}$.
- A significant analyzing power exists in the Coulomb-Nuclear Interference region.
- Recoil comes out almost perpendicular to the beam direction.

A. Poblaguev et al., Phys. Rev. D 79, 094014 (2009)

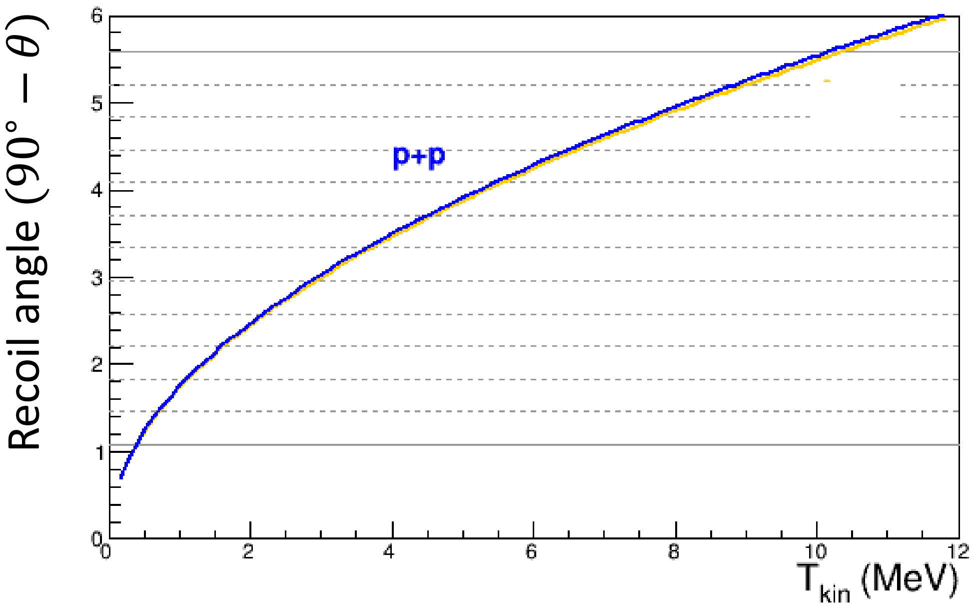

Kinetic energy of the recoil proton

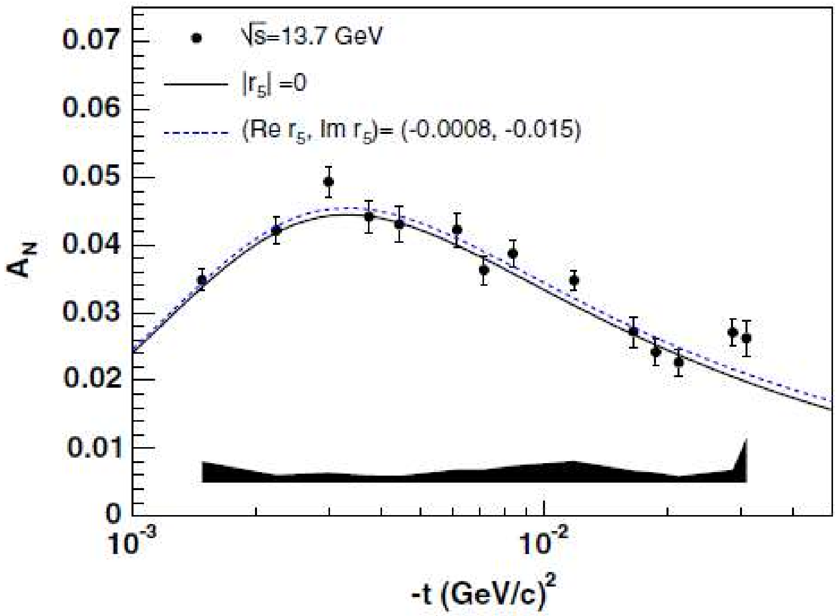

An Absolute Polarimeter at RHIC / EIC

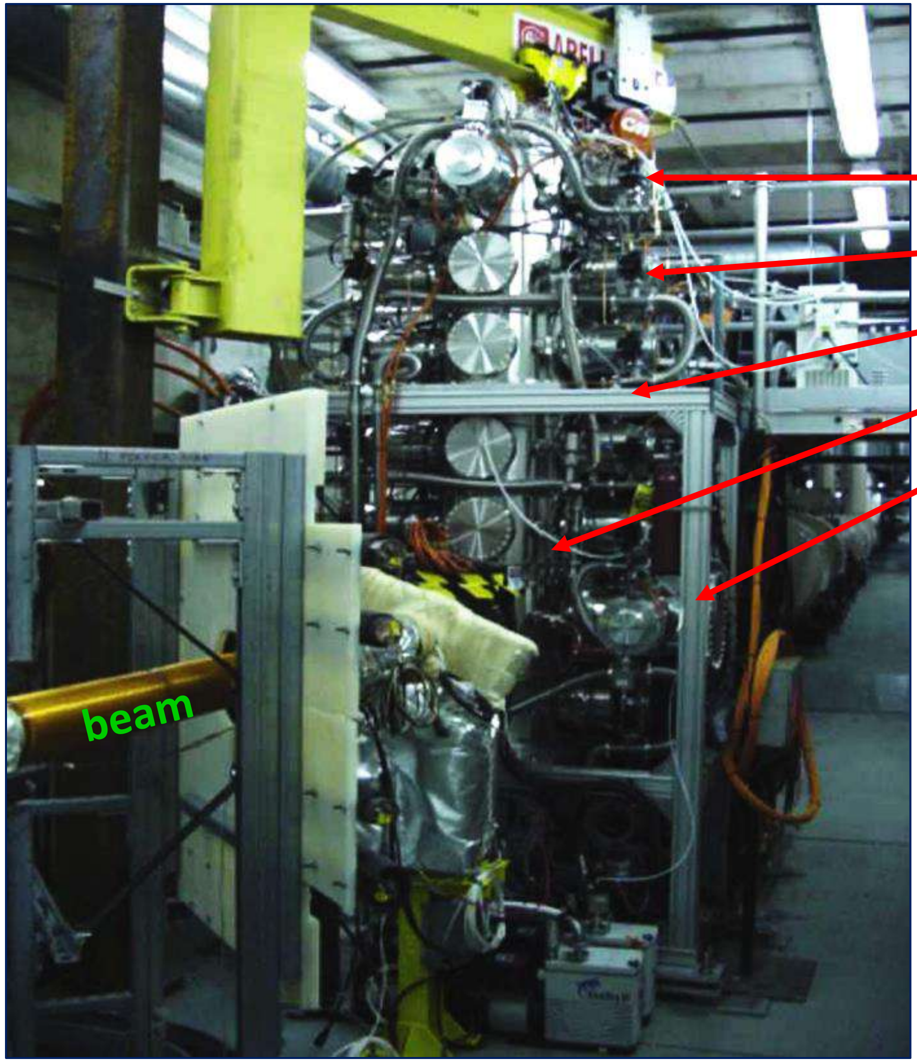

- H_2 source
- Dissociator
- RF unit
- Holding field
- Detectors

- **Polarized atomic hydrogen jet target (HJET)**

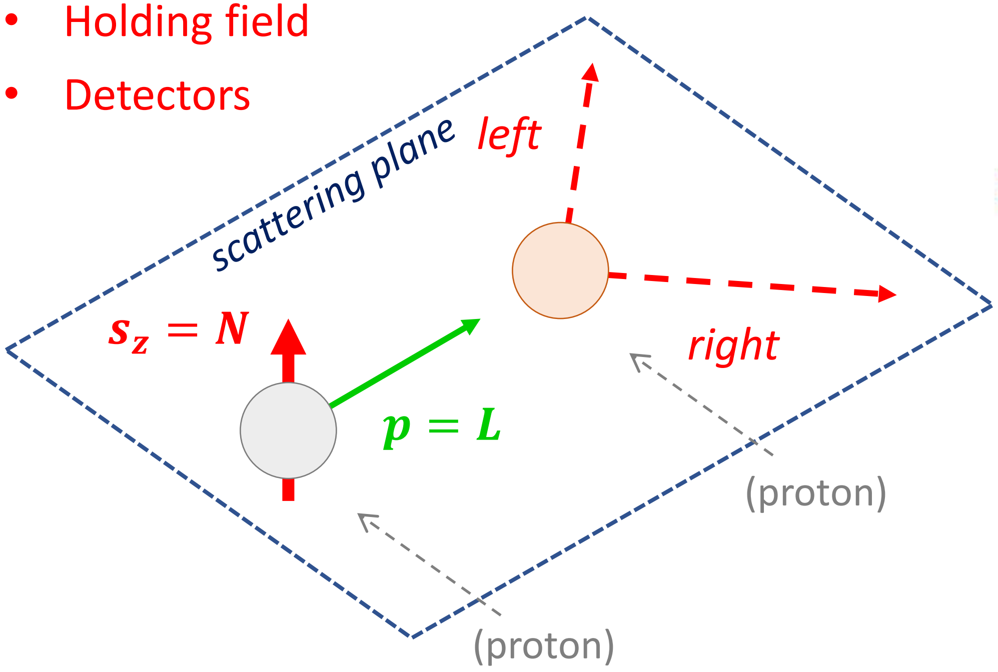

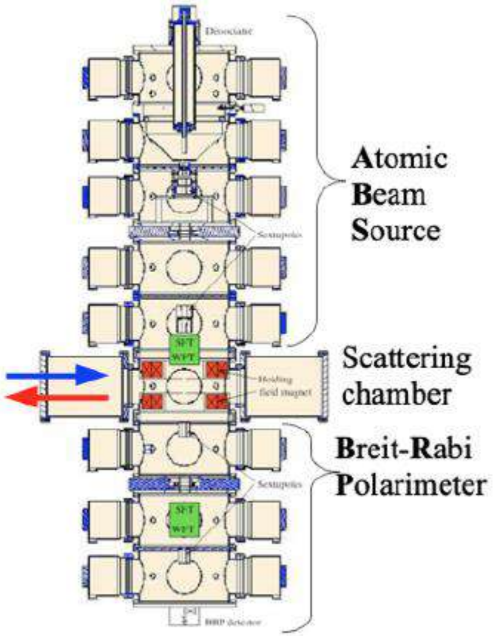

HJET Setup for RHIC / EIC

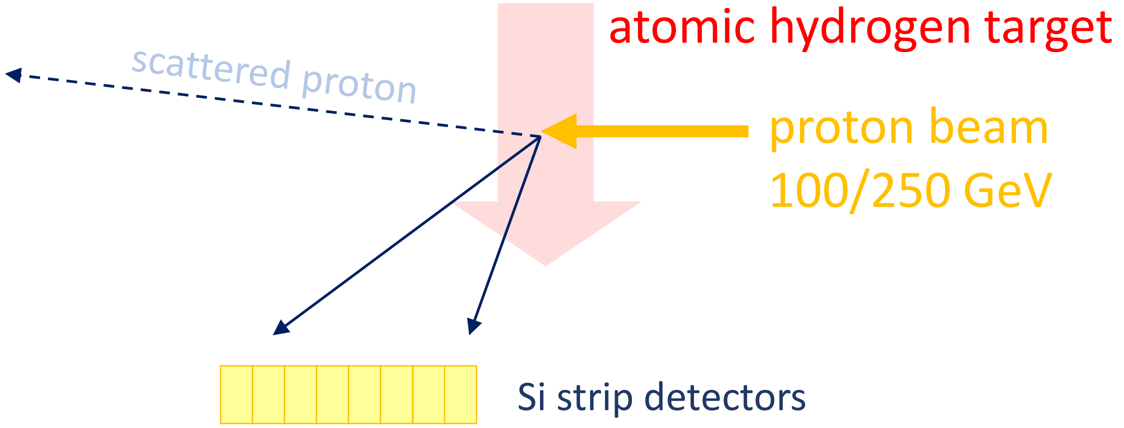

- Polarized atomic hydrogen jet target
- Set of eight Hamamatsu Si strip detectors
- 12 vertical strips
  - 3.75 mm pitch
  - 500 μm thick
- Uniform dead layer ≈ 1.5 μm

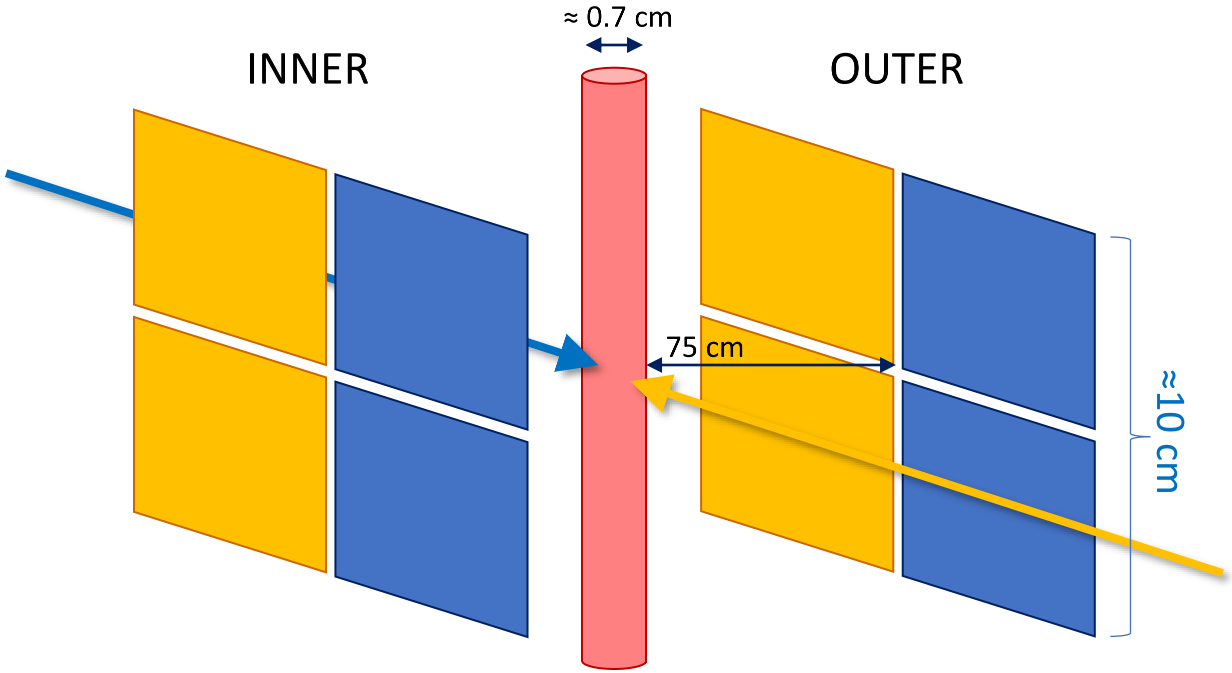

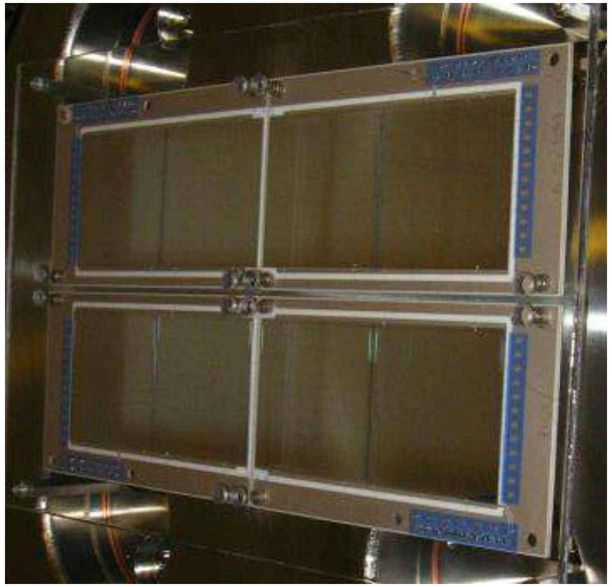

Absolute Beam Polarization

$$\varepsilon = A_N \cdot P$$

$$P_{Beam} = \frac{\varepsilon_{Beam}}{\varepsilon_{Target}} P_{Target}$$

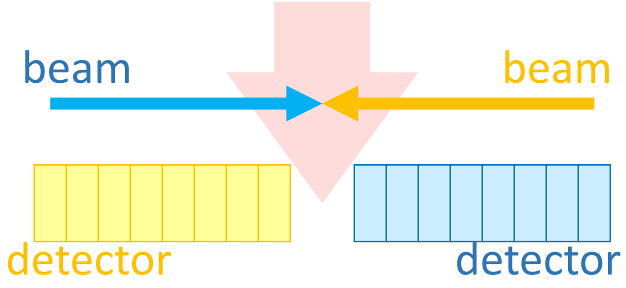

1

Polarization independent background

$$\varepsilon = \frac{N^{\uparrow} - N^{\downarrow}}{N^{\uparrow} + N^{\downarrow} + 2 \cdot N_{bg}} \Rightarrow \frac{\varepsilon_B}{\varepsilon_T} = \frac{N_B^{\uparrow} - N_B^{\downarrow}}{N_T^{\uparrow} - N_T^{\downarrow}}$$

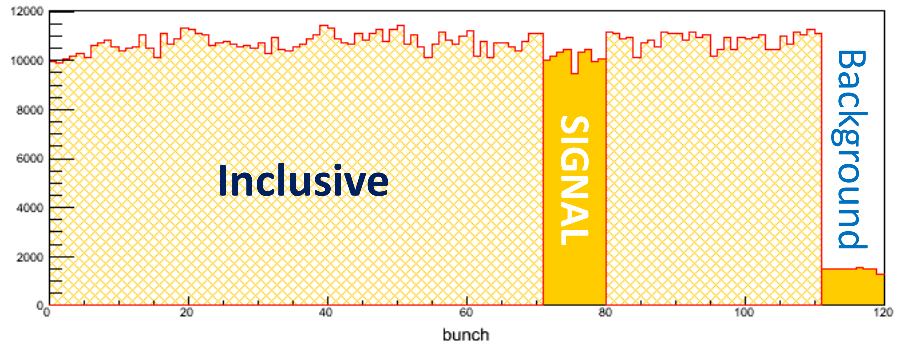

2

Polarization dependent background

$$\varepsilon = \frac{\varepsilon_{inc} - r \cdot \varepsilon_{bg}}{1 - r}$$

background fraction $r = N_{bg}/N$

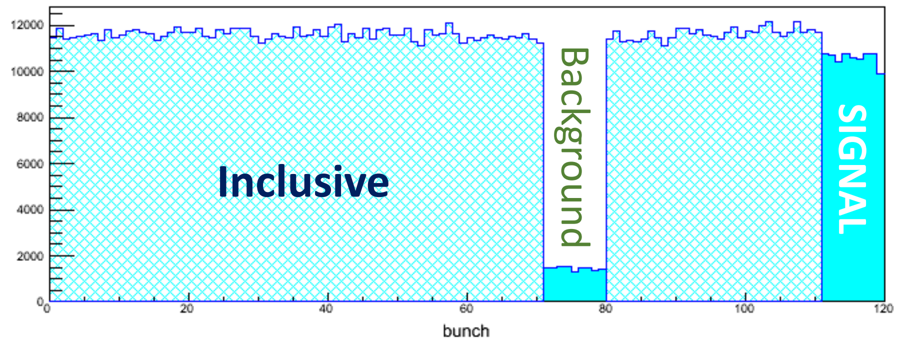

Measured Beam Polarizations

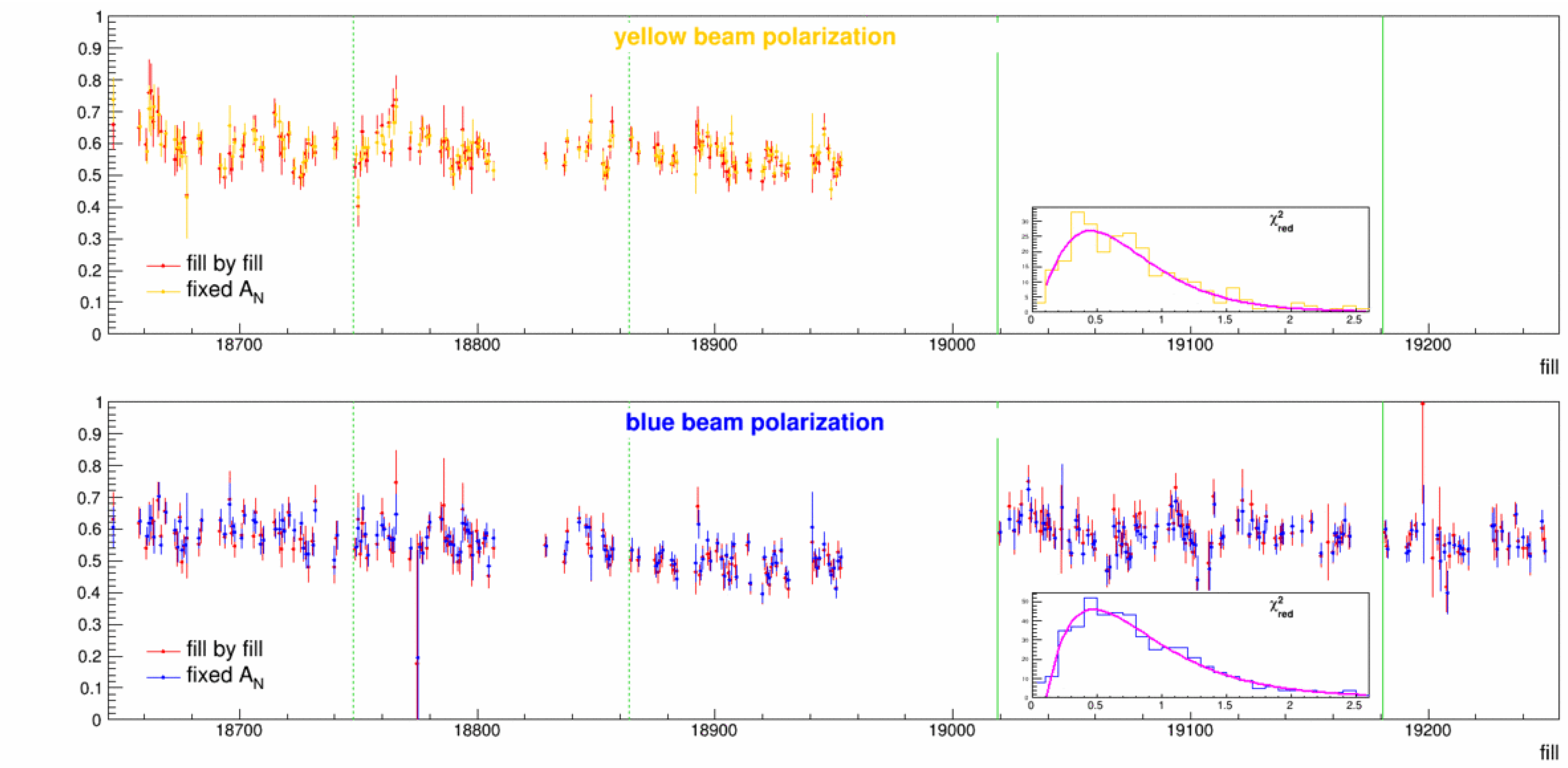

Additional Fast Polarimeters

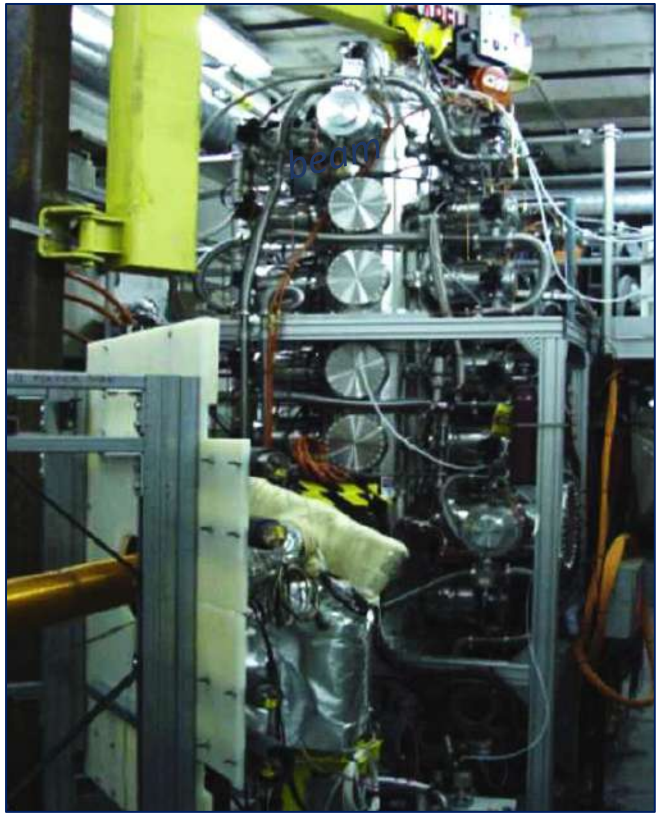

From our list of requirements:

Time-dependence (polarization decay)

Bunch-by-bunch polarization

Transverse polarization profile of bunches

Also has to be non-destructive!

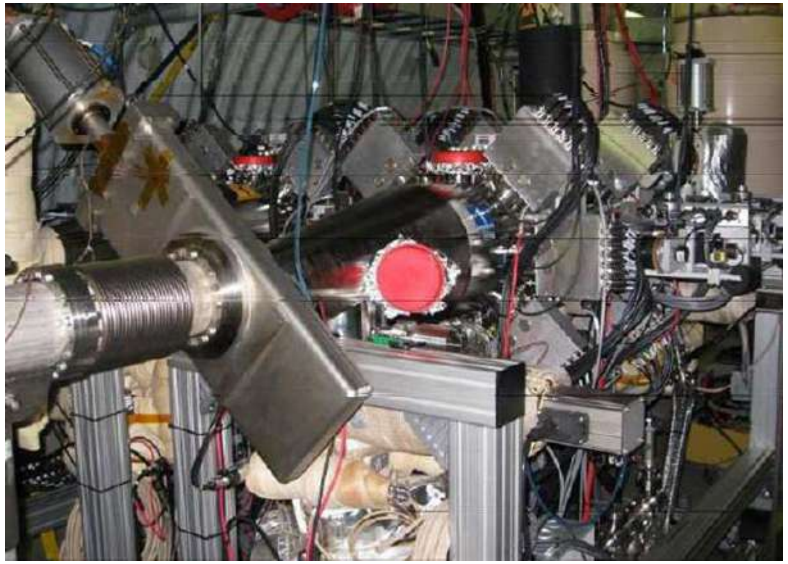

Carbon polarimeters

Fast measurement

$\delta P/P \approx 4\%$

Beam polarization profile

Bunch-by-bunch

Polarization decay (time dependence)

Hydrogen jet polarimeter

Polarized target

Continuous operation

$\delta P/P \approx 5-6\%$ per 8 hours of operation

normalization

Fiber Target Polarimeters

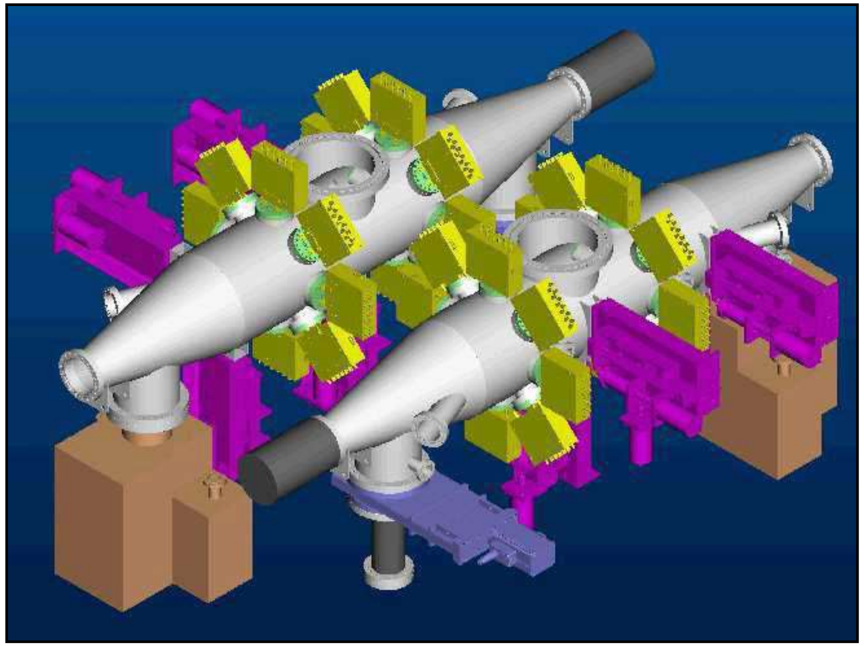

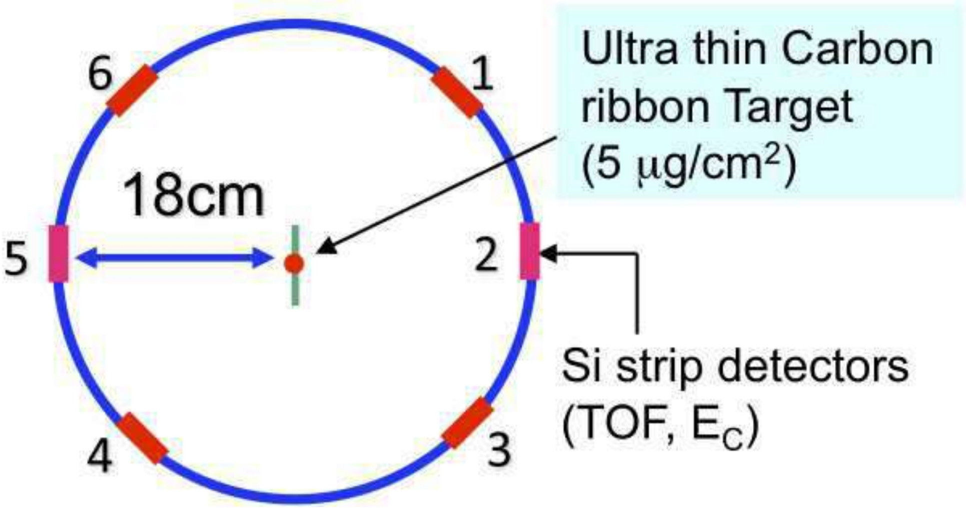

- Ultra-thin ribbon targets:

  $$\approx 10\ \mu m\ x\ 100\ \text{nm}$$

- Target holder inside the beam pipe

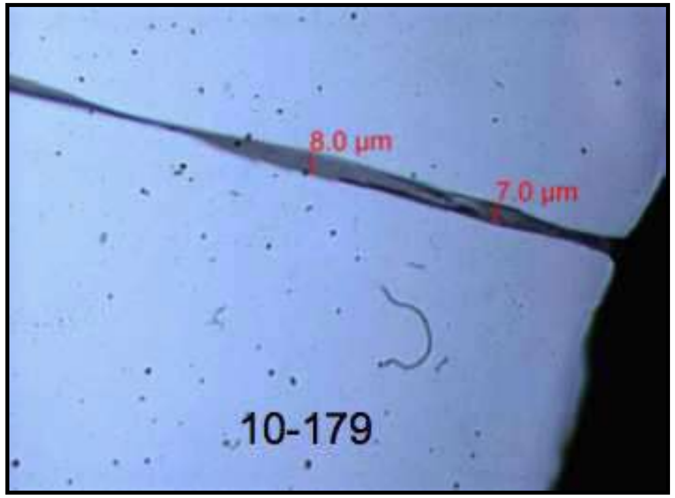

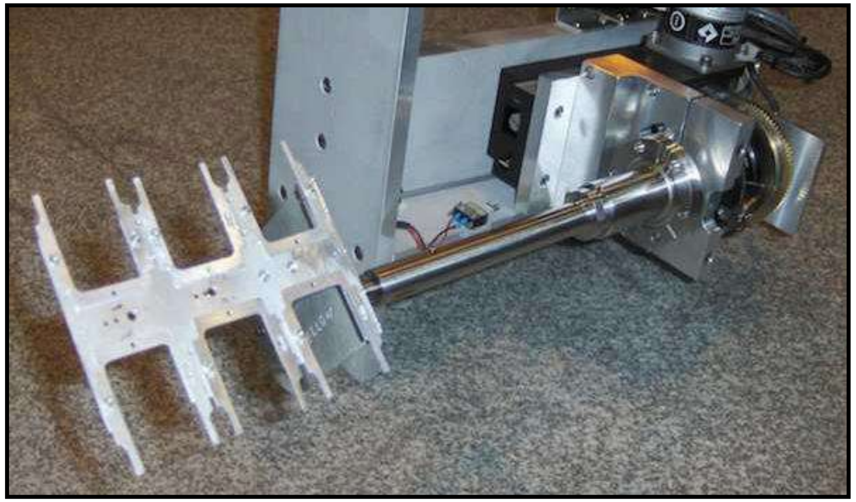

From RHIC to EIC

- Loss of increased asymmetry at lower energies, $A_N(-t)$
- Reduced bunch spacing requires much better understanding of background
    - Polarized or unpolarized
    - Better: reject/suppress background
    - Second detector layer to veto high energy particles

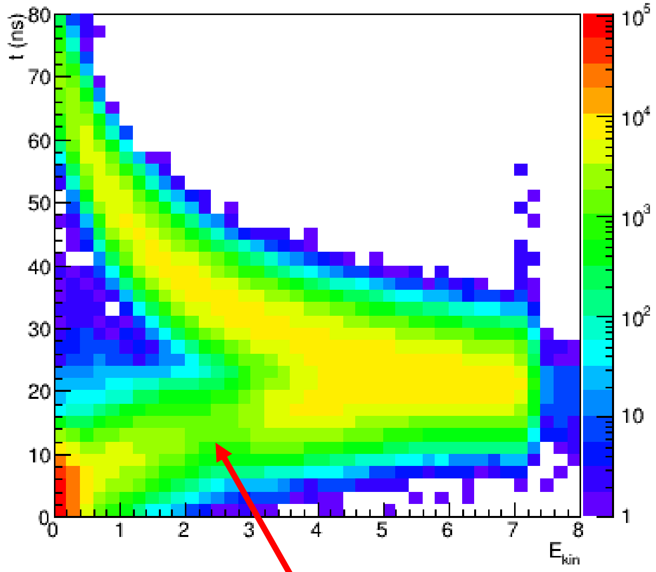

Punch through region

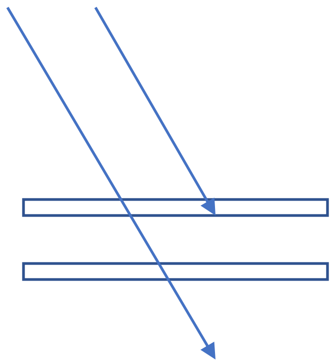

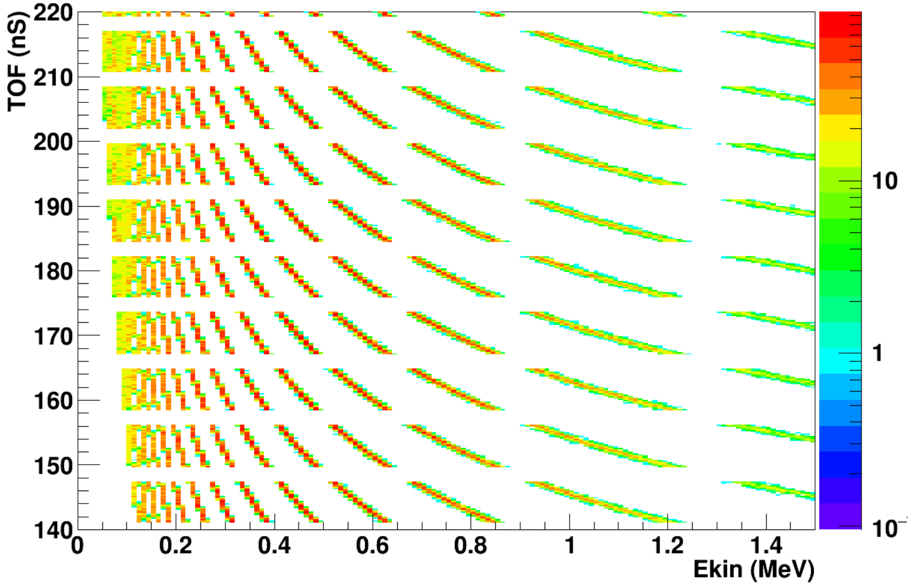

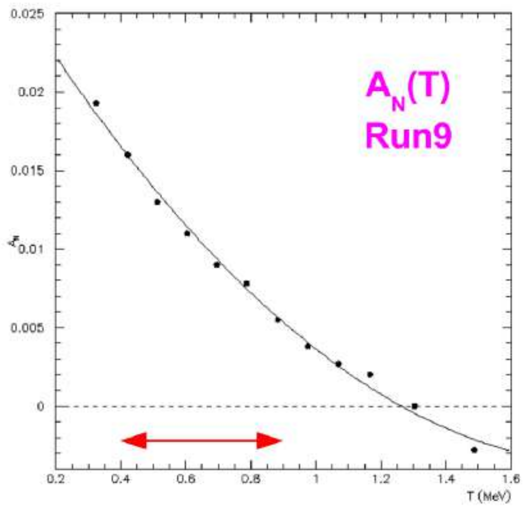

From RHIC to EIC

- Loss of increased asymmetry at lower energies, $A_N(-t)$
- Reduced bunch spacing requires much better understanding of background
  - Polarized or unpolarized
  - Better: reject/suppress background
- Increased beam current is problematic for the fiber target
  - Very limited cooling (radiation, thermal conductivity)
  - Sublimation temperature $T_{Carbon} \approx 2200° \; C$
  - Temperature saturates in a few ms

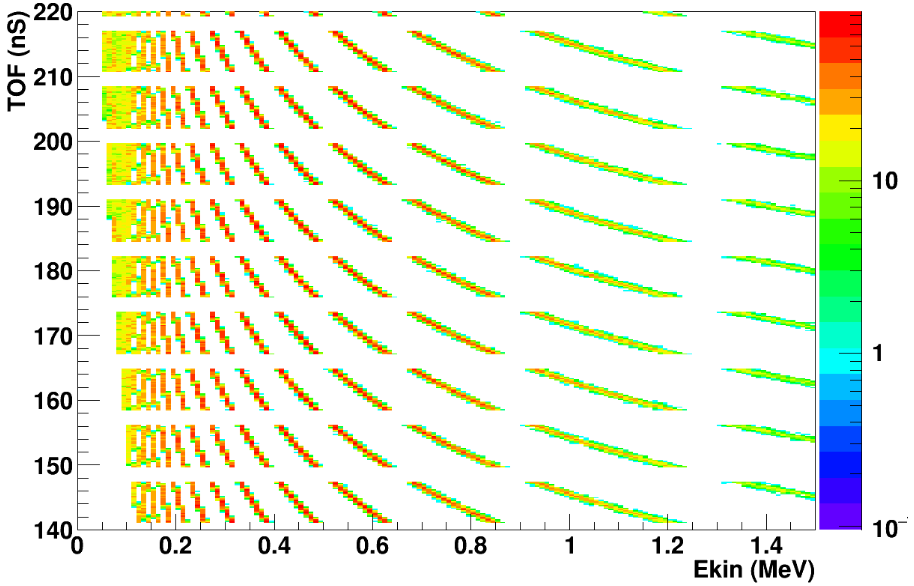

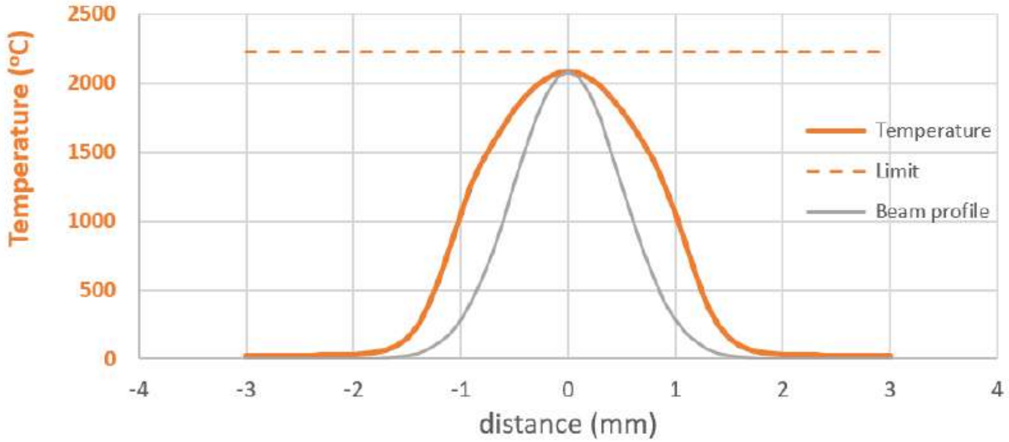

Can we find a target material that withstands higher temperatures?

Calculation by P. Thieberger, BNL

Outlook / Summary

Requirements and Delivery

	Polarized HJET	Unpolarized HJET	Carbon polarimeter	Forward neutrons
Absolute beam polarization	+	[+]	✖	[✖]
Polarization decay	[+]	+	+	+
Transverse profile	✖	✖	+	[✖]
Longitudinal profile	+	+	+	✖
Polarization vector	[✖]	+	+	+
Bunch polarization	✖	✖	+	✖

(*) Increased systematics

(*) A_N can be calculated, but needs to be confirmed; full background subtraction

(*) less accurate than pC

(*) depends on the target

(*) limited space for detectors with current magnet configuration

Recap: Hadron Polarimetry

- Proton beam energies: $50 - 275\ \mathrm{GeV}$
- Combination of devices for
    - Non-destructive
    - Absolute polarization
    - Fast measurements during store
    - Bunch profile
    - Local polarimetry at experiment
- Potential for future polarized light ion beams
    - Location allows for upgrades to the polarimeter setup

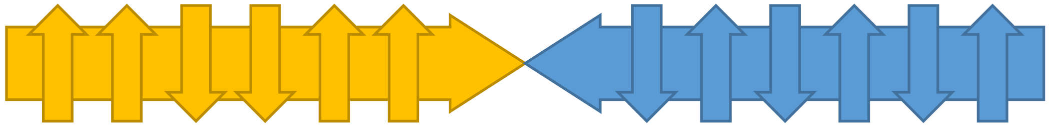

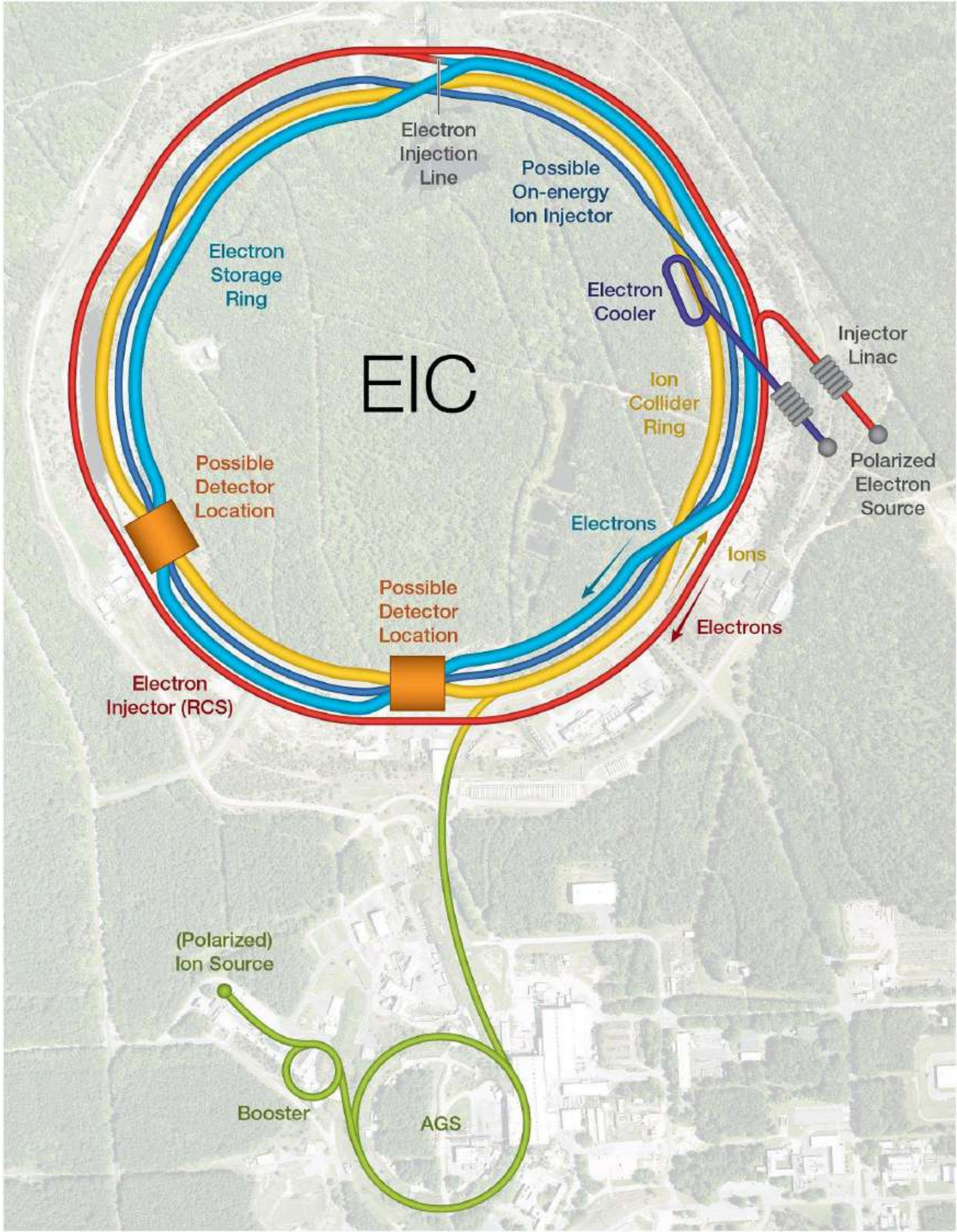

A Polarized Electron-Ion Collider

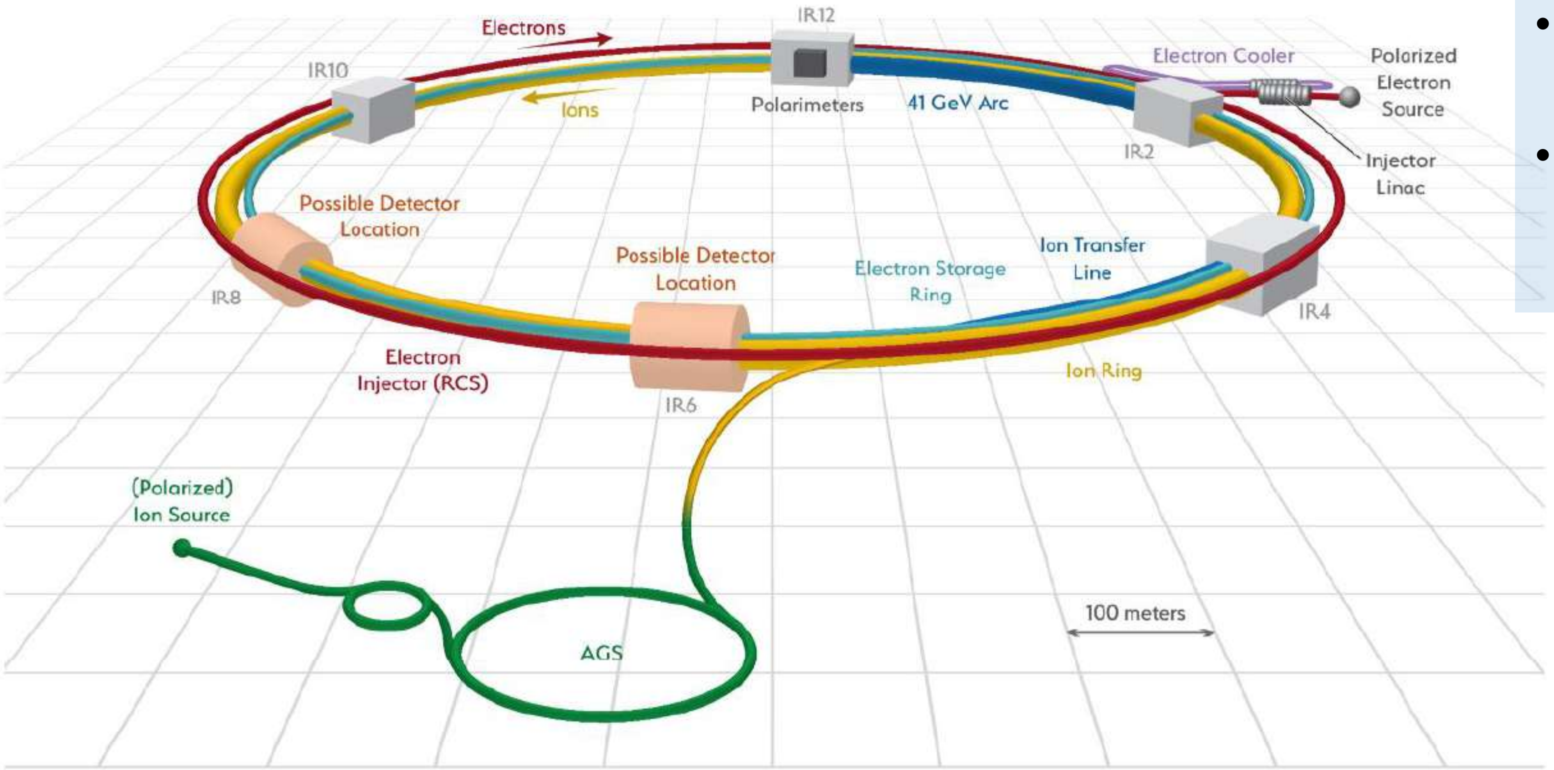

- **The EIC will be the first dedicated polarized electron-ion collider.**
- **Polarimetry is an integral part of the collider design to meet the demands of the physics goals.**